

DESY 85-110  
October 1985



THE TWO PHOTON RADIATIVE WIDTHS OF LIGHT MESONS AS A TEST OF GAUGE  
THEORIES WITH INTEGRALLY CHARGED QUARKS

by

J.H. Field

*Deutsches Elektronen-Synchrotron DESY*

ISSN 0418-9833

NOTKESTRASSE 85 2 HAMBURG 52

DESY behält sich alle Rechte für den Fall der Schutzrechtserteilung und für die wirtschaftliche Verwertung der in diesem Bericht enthaltenen Informationen vor.

DESY reserves all rights for commercial use of information included in this report, especially in case of filing application for or grant of patents.

To be sure that your preprints are promptly included in the  
HIGH ENERGY PHYSICS INDEX ,  
send them to the following address ( if possible by air mail ) :

DESY  
Bibliothek  
Notkestrasse 85  
2 Hamburg 52  
Germany

1. INTRODUCTION

The principal aim of the work presented here is to make a quantitative discrimination between models with fractional charge (FC) or integer charge (IC) quarks by using the wealth of experimental information [1] on the  $2\gamma$  widths of light mesons that has been obtained at  $e^+e^-$  storage rings in the last few years.

Tests, based particularly on the  $\eta'$   $2\gamma$  width  $\Gamma_{\gamma\gamma}(\eta')$ , have previously been proposed [2,3,4] and seem, at first sight, to strongly favour fractional quark charges. The theoretical assumptions which are crucial for these tests are critically examined in Sections 3.1 - 3.3.

The model for the radiative widths used in the present study, described in Section 3.4, is nonrelativistic quarkonium annihilation. Flavour mixing with glueball states is included. Allowance is made throughout for SU(3) breaking (i. e. effects due to the difference in the constituent masses of strange and non-strange quarks). Binding energy effects are included in the static limit, and for the pseudoscalars, the 1st order QCD correction.

In comparisons with experimental data only the ratios of radiative widths are considered, so relativistic corrections [5,6,7], which may be large in absolute value, should largely cancel. This is particularly true for the tensor mesons where the mass differences between  $f$ ,  $f'$  and  $A_2$  are small.

The essential predictions of gauge IC models for the  $2\gamma$  radiative widths of mixed quarkonium gluonium mesons are summarised in Section 2.

The flavour mixing of the ground state isospin zero pseudoscalar  $\eta(548)$ ,  $\eta'(958)$ ,  $\iota(1450)$  and tensor ( $f(1270)$ ,  $f'(1515)$ ,  $\theta(1720)$ ) states is described by a linear mass matrix in a non-strange quarkonium ( $ns>$ ), strange quarkonium ( $ss>$ ) gluonium ( $gg>$ ) basis. This model, presented in Section 4, is similar to that previously considered by Schmitzer [8], Rosner [9], and Rosner and Tuan [10]. The most important difference is that here SU(3) breaking corrections, as suggested by QCD ideas, and previously considered in [11, 12] are incorporated. The symmetry break-

THE TWO PHOTON RADIATIVE WIDTHS OF LIGHT MESONS AS A TEST OF GAUGE THEORIES WITH INTEGRALLY CHARGED QUARKS

Abstract

A test is made of the quark charges using the recently measured  $2\gamma$  widths of the pseudoscalar ( $\pi^0$ ,  $\eta$ ,  $\eta'$ ) and tensor ( $A_2$ ,  $f$ ,  $f'$ ) mesons. The model for  $\Gamma_{\gamma\gamma}$  is nonrelativistic quarkonium annihilation, including binding and SU(3) breaking corrections. The flavour mixing between the states ( $\eta$ ,  $\eta'$ ,  $\iota(1450)$ ) or ( $f$ ,  $f'$ ,  $\theta(1720)$ ) is given by a linear quarkonium gluonium mass matrix which includes mass dependent SU(3) breaking corrections.

For the pseudoscalars a fit is made to 5 experimental quantities sensitive to flavour mixing but independent of the quark charges. The best fit indicates a significant gluonium amplitude  $\approx 0.6$  in the  $\eta'$ . The integral charge quark model is consistent with the measured value of  $\Gamma_{\gamma\gamma}(\eta')$  only for effective gluon masses  $< 1.0 \text{ MeV}/c^2$  (95 % C.L.). Corrections from radial excitations are discussed and it is concluded that a pure quarkonium radial excitation interpretation of the  $\iota$  is unlikely.

In the fractional charge model the measurements of  $\Gamma_{\gamma\gamma}(f, f', A_2)$  indicate that the  $f$  and  $f'$  are almost ideally mixed quarkonium states. In gauge integer charge models charged gluon annihilation may give large contributions to  $\Gamma_{\gamma\gamma}(f, f')$ . Such models are excluded by constraints from the strong decays  $f, f' \rightarrow \pi\pi$ ,  $KK$  and the experimental upper limit on  $\Gamma_{\gamma\gamma}(\theta)BR(\theta \rightarrow KK)$ . Comparison of the fitted SU(3) breaking parameters with perturbative QCD expectations suggests  $\Lambda = 100 \pm 50 \text{ MeV}/c$ .

ing is found to be large, and to change essentially the predictions of such a model.

The analysis of the pseudoscalar mesons is presented in Section 5. The measured values of the  $1\Upsilon$  transition widths:

$$P(V) \rightarrow V(P)\Upsilon, J/\psi \rightarrow P\Upsilon \quad (P = \eta, \eta'; V = \rho, \omega, \phi)$$

the forward cross section ratio:

$$\sigma(\pi^+ \pi^- \rightarrow \eta\eta) / \sigma(\pi^+ \pi^- \rightarrow \eta' \eta')$$

and the ratio of decay widths:

$$\Gamma_{\eta\pi}(A_2) / \Gamma_{K\bar{K}}(A_2)$$

all of which are sensitive to the flavour wave functions of  $\eta, \eta'$  are used in a global fit to determine the non-strange ( $x$ ) and strange ( $y$ ) quarkonium amplitudes in the  $\eta$  and  $\eta'$ . Using these amplitudes in the quarkonium formula for the  $\eta'$  width, the predicted values of  $\Gamma_{\Upsilon\Upsilon}(\eta')$  in the FC and IC models are compared with the experimental measurement. Also predicted are the gluonium amplitudes in  $\eta, \eta', \chi, \chi'$ ;  $BR(J/\psi \rightarrow 1\Upsilon)$ ,  $BR(1 \rightarrow K\bar{K}\pi)$ ,  $\Gamma_{\Upsilon\Upsilon}(1), \Gamma_{\Upsilon\Upsilon}(\pi^0)$  and  $\Gamma_{V\Upsilon}(1), V = \rho, \omega, \phi$ .

A brief discussion is also given in Section 5 of corrections to the ground state model used here from mixing with radial excitations, and of the possibility of describing the  $1(1450)$  as a radially excited pure quarkonium state.

The tensor mesons are considered in Section 6. Here the measured radiative width ratios:

$$\Gamma_{\Upsilon\Upsilon}(f) / \Gamma_{\Upsilon\Upsilon}(A_2), \quad \Gamma_{\Upsilon\Upsilon}(f') / \Gamma_{\Upsilon\Upsilon}(A_2)$$

suffice to completely determine the mass matrix for the  $(f, f', \theta)$  system.

The flavour wave functions are checked by comparing with the experimental values the predictions for:

$$\Gamma_{\eta\pi}(f), \Gamma_{K\bar{K}}(f), \Gamma_{\pi\pi}(f'), \Gamma_{K\bar{K}}(f')$$

given by a model [13] based on OZI rule conserving amplitudes. The same model is used for  $\Gamma_{\eta\pi}(A_2), \Gamma_{K\bar{K}}(A_2)$  to constrain the non-strange quark content of the  $\eta$  and to predict several other strong decay widths:

$$\Gamma_{pp}(T), \Gamma_{p\Upsilon}(T) \quad \text{where } T = K^{*0}(1430), A_2$$

For the IC model, where the measured radiative widths predict large gluonium amplitudes in the physical  $f, \theta$ , a further constraint on the flavour wavefunction is provided by the experimental value [14] of:

$$\Gamma_{\Upsilon\Upsilon}(\theta) BR(\theta \rightarrow K\bar{K})$$

In the IC model analysis the possibly large contributions of charged gluonium annihilation amplitudes to the two photon radiative widths are taken into account.

A critical discussion of the models used and the results obtained, particularly in relation to similar related work, is given in Section 7. Other recent tests of the gauge IC models using  $2\Upsilon$  interactions are also briefly mentioned.

## 2. GAUGE INTEGRAL CHARGE QUARK MODELS

The 'naive' IC model as originally proposed by Han and Nambu [15] is already ruled out by measurements of high transverse momentum jet production in tagged photon-photon collisions [16,17] as well as by a recent experiment [18] that observed the direct production of photons in  $\gamma\gamma e^+e^-$  annihilation into hadrons. There exists however a class of gauge models which unify the strong, weak and electromagnetic interactions [19-23] where the electric charge of quarks depends upon the  $q^2$  (i. e.  $-(\text{mass})^2$ ) of the photon probe:

$$Q_{\alpha i} = Q_i^{(0)} + \left[ \frac{m_g^2}{m_g^2 + q^2} \right] Q_{\alpha}^{(8)} \quad (1)$$

Here  $i, \alpha$  are labels for flavour and colour.  $Q_i^{(0)}$  is a colour singlet flavour dependent charge with fractional values:

$$\begin{aligned} Q_i^{(0)} &= 2/3 & i &= u, c, \dots \\ &= -1/3 & i &= d, s, b, \dots \end{aligned} \quad (2)$$

$Q_{\alpha}^{(8)}$  is a flavour singlet, colour octet, charge expressed as a vector in colour space as:

$$\vec{Q}^{(8)} = (-2/3, 1/3, 1/3) \quad (3)$$

$m_g$  is the effective gluon mass which is generated by spontaneous symmetry breaking of the colour SU(3) symmetry. The propagator-like term in (1) results from the mixing of a massive neutral gluon with the photon. In some theories [22] there is a unique mass for all gluons, charged or neutral, while in others [23] only one neutral gluon and the charged gluons acquire (possibly different) masses. In the latter case the other neutral gluons remain massless, respecting an exact SU(2) colour symmetry. In general in such theories the electric charge of quarks has the  $q^2$  dependence shown in (1). The value of  $m_g$  is not determined by theory. If  $q^2 \gg m_g^2$  the colour octet charge is suppressed, so that the effective quark charge is the same as in the standard FC model. On the other hand, if  $q^2 \ll m_g^2$  the effective quark charges become those of the Han Nambu model:

$$\begin{aligned} \vec{Q}_i &= (0 \ 1 \ 1) & i &= u, c, \dots \\ &= (-1 \ 0 \ 0) & i &= d, s, b, \dots \end{aligned} \quad (4)$$

As in (3) the vectors are in colour space.

The published measurements of tagged jet production [16,17] have been shown to be consistent with the expression (1) for the quark charge, provided that:

$$m_g \lesssim 200 \text{ MeV}/c^2.$$

In jet production allowance has to be made for the contribution of charged gluons. The gluon electric charge is a pure octet of colour. However, additional kinematic terms in the cross section proportional to  $q^2/m_g^2$  cancel the propagator factor in (1) when  $q^2 \gg m_g^2$  to give a non-vanishing cross section in this limit, unlike for the case of the quark colour octet charge [24]. Similar behaviour may be expected in the  $2\gamma$  width of a meson from any charged gluon contribution in its wave function, but no explicit calculations have been made to date.

The two photon radiative width of a meson in the quarkonium annihilation model (see Section 3.4 below) is proportional to the square of an amplitude which contains as a factor the colour singlet projection of the square of the quark charge  $(1/\sqrt{3}) Q_i^2$ , where:

$$Q_i^2 = \sum_{\alpha} \left\{ \left[ Q_i^{(0)} \right]^2 + \frac{m_g^4}{(m_g^2 + q_1^2)(m_g^2 + q_2^2)} \left[ Q_{\alpha}^{(8)} \right]^2 \right\} \quad (5)$$

The possibility to observe the colour octet charge  $Q_{\alpha}^{(8)}$ , below the threshold for excitation of colour has been questioned by Lipkin [27]. Lipkin's objections (based on the existence of colour oscillations between the two quark photon vertices in a  $\gamma\gamma \rightarrow q\bar{q}$  amplitude, which add non-diagonal terms to the colour sums in (5)) are not universally accepted [24-26]. It is however suggested in [27] that the  $2\gamma$  widths of pseudoscalar quark-

onium states may still allow experimental sensitivity to the colour octet quark charge below threshold. This is because such widths are governed, in current algebra language, by the axial anomaly [28,29] which probes the short distance (high energy) behaviour of the quark currents. Similar behaviour may be expected in the quarkonium annihilation model used in this paper, as it is equivalent, in constituent quark language, to the current algebra calculation of  $\Gamma_{\gamma\gamma}(\pi^0)$  [29]. The validity and predictive power of the latter for the heavier pseudoscalar mesons  $\eta, \eta'$  is discussed in some detail in Section 3.3 below.

The colour singlet projection of the charged squared operator for gluons in an IC theory is, in the limit  $q_1^2, q_2^2 \ll m_g^2, \sqrt{2}$  (4 of the 8 coloured gluons have charge  $\pm 1e$ ). Comparing this with the value of  $Q_1^2$  given in Table 1 for the different quark flavours in the FC and IC models, it is clear that charged gluons can give an important contribution to the  $2\gamma$  widths of mixed quarkonium-gluonium states. This is the same as saying that discrimination between the FC and IC models using the  $2\gamma$  widths of such states first requires knowledge of the quarkonium and gluonium amplitudes in them. These amplitudes are determined in the following analysis using a linear mass matrix for the  $(\eta, \eta', \iota)$  or  $(f, f', \theta)$  systems, together with phenomenological constraints (ratios of  $1\gamma$  or strong transition widths) that are independent of the quark or gluon charges.

Measurements of  $2\gamma$  radiative widths at  $e^+e^-$  colliders which use virtual photons cannot definitively exclude gauge IC models. They rather set a very low (in the untagged case) upper limit on the parameter  $m_g$  of the theory. Definite exclusion of the IC model requires experiments using processes involving the coupling of two real photons. Two recent examples are mentioned in Section 7 below. In the following if the IC and FC models are compared without qualification it is tacitly assumed that  $m_g^2 \gg \langle q^2 \rangle$  so that the propagator suppression factor in (5) is not operative. Quantitative estimates of the upper limit on  $m_g$  require for mixed quarkonium-gluonium states knowledge of the dynamics of the process  $g^+g^- \rightarrow \gamma\gamma$ . In Section 5 an upper limit on  $m_g$  is found on the assumption that the  $\eta'$  radiative width is dominated by quarkonium annihilation. This is justified because the wave function at the origin vanishes for  $g^+g^-$  in a  $0^-$  state. For the tensor mesons, on the contrary, the S-wave state is allowed (forbidden) for  $g^+g^-$  ( $q\bar{q}$ ). The possible dominance of the  $g^+g^-$

annihilation contribution is taken into account in the analysis of the tensor mesons in the IC model presented below in Section 6.2.

### 3. MODELS FOR THE $2\gamma$ RADIATIVE WIDTHS OF LIGHT MESONS

Before presenting the quarkonium annihilation model to be used subsequently in this paper, a brief critical review is given of other models for the  $2\gamma$  widths of mesons. In particular the relevance and possible sensitivity of these models to the determination of the quark charges is discussed. Although some of the models were proposed twenty or more years ago, it is only recently that experimental data of sufficient quality [1,2] to test their predictions has become available.

#### 3.1 Flavour SU(3) and Vector Meson Dominance (VDM)

This type of model, which relates the strong coupling constant  $f_{\rho\omega\pi}$  to the electromagnetic decays:

$$\rho, \omega \rightarrow e^+e^-, \omega \rightarrow \pi^0\gamma, \pi^0 \rightarrow \gamma\gamma$$

was proposed by Gell-Mann, Sharp and Wagner [30]. The amplitudes for these processes are represented by the diagrams shown in Fig. 1, where the notation for the coupling constants  $f_{\rho\omega\pi}$ ,  $f_{\rho\gamma}$ ,  $f_{\omega\gamma}$  is defined. The transitions  $\omega \rightarrow \pi^0\gamma$ ,  $\pi^0 \rightarrow \gamma\gamma$  are related to  $f_{\rho\omega\pi}$  by VDM couplings of 1, 2 photons respectively:

$$\Gamma_{e^+e^-}(V) = \alpha^2 C_{V\gamma}^2 f_V^2 \quad (6a)$$

$$\Gamma_{\pi^0\gamma}(\omega) = \frac{\alpha}{96} \frac{[m_\omega^2 - m_{\pi^0}^2]^3}{m_\omega^3} f_{\rho\gamma}^2 f_{\rho\omega\pi}^2 \quad (6b)$$

$$\Gamma_{\gamma\gamma}(\pi^0) = \frac{\alpha^2}{192} \frac{3}{m_\pi} f_{\rho\gamma}^2 f_{\omega\gamma}^2 f_{\rho\omega\pi}^2 \quad (6c)$$

$$\text{where } V = \rho, \omega, \quad C_\rho = \frac{1}{12}, \quad C_\omega = \frac{1}{36}.$$

The dependence of the couplings on the photon (mass)<sup>2</sup> and other mass extrapolations are neglected throughout in this model.

Using the experimental values of  $\Gamma_{e^+e^-}(\rho)$ ,  $\Gamma_{e^+e^-}(\omega)$ ,  $\Gamma_{\pi^0\gamma}(\omega)$  [31], (6a-c) give:

$$\Gamma_{\gamma\gamma}(\pi^0) = 11 \pm 2 \text{ eV}$$

to be compared with the experimental value [31]

$$\Gamma_{\gamma\gamma}(\pi^0) = 7.95 \pm 0.55 \text{ eV.}$$

The model of Ref. [30] was generalised to the case of the  $\eta$ ,  $\eta'$  mesons by Dalitz and Sutherland [32] \*. Defining the SU(3) octet-singlet mixing angle  $\theta$  for the  $\eta$ ,  $\eta'$  by:

$$\eta = \eta_8 \cos\theta - \eta_1 \sin\theta \quad (7a)$$

$$\eta' = \eta_8 \sin\theta + \eta_1 \cos\theta \quad (7b)$$

it is found that

$$\Gamma_{\gamma\gamma}(\eta')/\Gamma_{\gamma\gamma}(\pi^0) = \frac{\cos^2\theta}{3} \left[ \tan\theta + 2R \right]^2 (m_{\eta'}/m_{\pi^0})^3 \quad (8a)$$

$$\Gamma_{\gamma\gamma}(\eta)/\Gamma_{\gamma\gamma}(\pi^0) = \frac{\cos^2\theta}{3} \left[ 1 - 2R \tan\theta \right]^2 (m_{\eta'}/m_{\pi^0})^3 \quad (8b)$$

where  $R$  is the amplitude ratio  $A(\eta_1 \rightarrow \rho\gamma)/A(\eta_8 \rightarrow \rho\gamma)$ . The parameters  $\theta$ ,  $R$  may be determined from the ratios of the  $1\gamma$  transition widths:

$$\Gamma_{\rho\gamma}(\eta')/\Gamma_{\pi^0\gamma}(\omega) = \left[ \frac{m_{\eta'}^2 - m_\rho^2}{m_\omega^2 - m_\pi^2} \right]^3 \left[ R \cos\theta + \sin\theta \right]^2 \quad (9a)$$

$$\Gamma_{\eta\gamma}(\rho)/\Gamma_{\pi^0\gamma}(\omega) = \frac{1}{3} \left[ \frac{m_\rho^2 - m_\eta^2}{m_\omega^2 - m_\pi^2} \right]^3 \left[ \cos\theta - R \cos\theta \right]^2 \quad (9b)$$

\* There is a sign error in (12b) of this reference.  $-\frac{A}{3} + \frac{A}{3}$ . The R.H.S. of (13b) then becomes simply 0.084. Also a factor  $(m_{\eta'}/m_{\pi^0})^3$  is missing on the R.H.S. of (17).

Using the world average value of  $\Gamma_{\gamma\gamma}(\eta')$  (see Section 5 below) and the branching ratio for  $\eta' \rightarrow \gamma\gamma$  from [31], the full width of the  $\eta'$  is found to be:

$$\Gamma_{\eta'} = 240 \pm 30 \text{ keV}$$

Taking other full widths and branching ratios from [31], the decay widths in (9) are:

$$\Gamma_{\rho\gamma}(\eta') = 72 \pm 8 \text{ keV}$$

$$\Gamma_{\pi^0\gamma}(\omega) = 861 \pm 56 \text{ keV}$$

$$\Gamma_{\eta\gamma}(\rho) = 55 \pm 16 \text{ keV}$$

Solving (9a,b) for  $\Theta$ ,  $R$  then gives:

$$R = 1.22 \pm 0.22 \quad \Theta = -13^\circ \pm 6^\circ$$

Eqns (8a,b) and the experimental value of  $\Gamma_{\gamma\gamma}(\pi^0)$  then predict:

$$\Gamma_{\gamma\gamma}(\eta') = 4.4 \text{ keV}$$

$$\Gamma_{\gamma\gamma}(\eta) = 0.41 \text{ keV}$$

which may be compared with the experimental values (see Section 5 below):

$$\Gamma_{\gamma\gamma}(\eta') = 4.5 \pm 0.4 \text{ keV}$$

$$\Gamma_{\gamma\gamma}(\eta) = 0.56 \pm 0.08 \text{ keV}$$

This purely SU(3) calculation is in moderately good agreement with experiment for  $\pi^0$ ,  $\eta$  and  $\eta'$ . The quark model and the nonet symmetry assumption (see Section 3.3 below) further predict  $R = \sqrt{2}$  in good agreement with the value found above. Since however the quark concept is not used in the pure SU(3) calculation it sheds no light whatever on the question of the quark charges.

### 3.2 The Model of Van Royen and Weisskopf

Van Royen and Weisskopf [33] were among the first authors to use quark properties in a detailed way to calculate radiative transition

rates. The essential features of the transition amplitudes in the model are shown in Fig. 2.

The process  $V \rightarrow e^+e^-$  is mediated by the quark annihilation diagram (Fig. 2a). In this non-relativistic model the  $q\bar{q}$  state  $V$  is described by a single parameter, the wave function at the origin  $\psi_V(0)$ . The decays  $V(P) \rightarrow P(V)\gamma$  are single quark spin flip (magnetic dipole) transitions, whose strength is parameterised by the quark transition moment  $\mu_P$  (Fig. 2b). Two diagrams with  $q$  (or  $\bar{q}$ ) spin flip contribute. The amplitude for  $P \rightarrow \gamma\gamma$  (Fig. 2c) is the product of the amplitudes of Figs. 2a, b. There are 4 such amplitudes corresponding to  $q$  ( $\bar{q}$ ) spin flip and to exchange of the photons. Taking into account flavour mixing in the  $V$ ,  $P$  wave functions, the radiative widths for the processes in Figs. 2a, b, c are [12]:

$$\Gamma_{e^+e^-}(V) = \frac{16\pi\alpha^2}{M_V^2} \left| \sum_i Q_i A_i^V \psi_V(0) \right|^2 \quad (10a)$$

$$\Gamma_{P\gamma}(V) = \frac{4\alpha}{3} k_{VP}^3 \left| \sum_i V_i A_i^P \frac{Q_i}{m_i} \mu_i I_i \right|^2 \quad (10b)$$

$$\Gamma_{\gamma\gamma}(P) = 4\alpha k_{PV}^3 \left| \sum_i V_i A_i^P \frac{Q_i}{m_i} \mu_i I_i \right|^2$$

$$\Gamma_{\gamma\gamma}(P) = 12\pi\alpha^2 M_P^3 \left| \frac{\sum_i \sum_j V_i A_j^P Q_i}{V} \mu_i I_i \right|_{M_V}^{-3/2} \quad (10c)$$

$$\times \left| \sum_i Q_i A_i^V \psi_V(0) \right|^2$$

where  $k_{VP} = (M_V^2 - M_P^2)/2 M_V$ .

Here  $Q_i$  is the colour averaged quark charge for flavour  $i$ ,  $\mu_i$  is the effective quark moment (= 1 for a Dirac Quark) and  $I_i$  is the overlap integral between the  $P$  and  $V$  spatial wave functions. The SU(3) symmetry limit is given by setting all flavour dependent parameters, with the exception of the quark charges, to constant values.



Because of the factorisable form of the amplitude in (10c)  $\Gamma_{\gamma\gamma}(P)$  may be expressed entirely in terms of  $\Gamma_{e^+e^-}(V)$  and  $\Gamma_{V\gamma}(P)$  or  $\Gamma_{P\gamma}(V)$ :

$$\Gamma_{\gamma\gamma}(P) = \frac{9M_P^3}{16\alpha} \left\langle \vec{V} \right| \frac{P}{\zeta_V} \left[ \frac{\Gamma_{P\gamma}(V)\Gamma_{ee}(V)}{k^3 M_V} \right]^{1/2} \left| 0 \right\rangle \quad (11)$$

If  $M_P > M_V$  the replacement

$$\Gamma_{P\gamma}(V) \rightarrow \Gamma_{V\gamma}(P)/3$$

is required.

The flavour amplitudes  $A_i^{P,V}$  are needed only to determine the sign coefficients  $\zeta_V^P$ . For an ideally mixed  $\phi$  and  $\omega$ :

$$\begin{aligned} |\phi\rangle &= |s\bar{s}\rangle \\ |\omega\rangle &= 1/\sqrt{2}(|u\bar{u}\rangle + |d\bar{d}\rangle) \end{aligned}$$

and arbitrary octet singlet mixing angle for  $(\eta, \eta')$ :

$$\zeta_\rho^\eta = \zeta_\omega^\eta = -\zeta_\phi^\eta = \zeta_\rho^{\eta'} = \zeta_\omega^{\eta'} = \zeta_\phi^{\eta'} = +1 \quad (12)$$

Substituting into (11) the measured values of

$$\Gamma_{ee}(V), \Gamma_{\rho\gamma}(\eta'), \Gamma_{\omega\gamma}(\eta'), \Gamma_{\eta\gamma}(\phi), \Gamma_{\eta\gamma}(\rho)$$

[31], and calculated values of  $\Gamma_{\eta\gamma}(\phi)$ ,  $\Gamma_{\eta\gamma}(\omega)$  (using (10b) and assuming ideally mixed  $\omega$ ,  $\phi$  and  $= -11^\circ$ ) the following values are obtained for the  $2\gamma$  widths:

$$\Gamma_{\gamma\gamma}(\pi^0) = 9.6 \pm 0.9 \text{ eV}, \Gamma_{\gamma\gamma}(\eta) = 0.79 \pm 0.22 \text{ keV}, \Gamma_{\gamma\gamma}(\eta') = 4.7 \pm 0.8 \text{ keV}$$

The errors quoted correspond only to the experimental errors on the radiative widths in (9). Good agreement is found, within these errors, with the experimental values given above.

If the decays  $P \rightarrow \gamma\gamma$  are indeed described, at the quark level, by (10c) there is no possibility to test the quark charges using these processes. The colour octet charge contributes only when the amplitude contains the colour sum of the squared quark charge operator for a given flavour. In (10c)  $Q_i, Q_i'$  are the results of independent colour sums for quarks of flavour  $i, i'$ . More directly it can be seen (Fig. 2c) that the amplitude factorises into two  $1\gamma$  transition vertices, linked by a colour singlet hadron propagator. Since however we expect from the asymptotic freedom of QCD that quarks will behave at short distances as free particles, there is perhaps little physical justification for an asymmetrical diagram as shown in Fig. 2c, where one photon is produced by a short distance  $q\bar{q}$  annihilation process, and the other by a non-annihilation spin flip transition which produces a far-off-shell virtual vector meson\*.

The idea that the  $P \rightarrow 2\gamma$  transition is itself a short distance  $q\bar{q}$  annihilation process, where the two photons appear in the amplitude in a symmetrical way is the basis of both the current algebra calculation of  $\Gamma_{\gamma\gamma}(\pi^0)$  and of the quarkonium annihilation model, to be used later in this paper, which will now be discussed in turn.

### 3.3 Current Algebra Estimation of $\Gamma_{\gamma\gamma}(P)$

The  $2\gamma$  radiative width of the  $\pi^0$  was calculated by Adler [29] using the PCAC equation, modified to take into account the contribution of the triangle anomaly diagrams [28]. Such a diagram is shown in Fig. 3a. The theory predicts complete dominance of  $\Gamma_{\gamma\gamma}(\pi^0)$  by these diagrams at the unphysical point where  $(q_1 + q_2)^2 = 0$ . An essential ingredient of the calculation is the extrapolation of the matrix element of the divergence of the axial vector current:

$$\langle \gamma(q_1)\gamma(q_2) | \frac{\partial A^\lambda}{\partial x^\lambda} | 0 \rangle$$

\* The authors of [33] in fact used the word 'quarkonium' to describe the  $\pi^0$ . They insisted, however, that the  $q\bar{q}$  pair should be strongly bound. In 1967 the concept of asymptotic freedom had yet to be invented.

from  $(q_1 + q_2)^2 = 0$  to  $m_{\pi^0}^2$ . Because  $m_{\pi^0}^2$  is small compared to a typical light hadron  $(\text{mass})^2$  of  $\approx 1$   $(\text{GeV}/c^2)^2$  one may hope that the neglect of this extrapolation is justified. It is found that:

$$\Gamma_{\gamma\gamma}(\pi^0) = \frac{\alpha^2 S_{\pi\pi}^2}{32\pi^3 f_\pi^2} \quad (13)$$

Here  $S_{\pi\pi}$  is  $\sum_{\alpha\beta} A_{\alpha\beta}^{\pi\pi} Q_{\alpha\beta}^2$  where  $A_{\alpha\beta}^{\pi\pi}$  is the amplitude of  $q_1 \bar{q}_1$  in the  $\pi^0$  wave function,  $Q_{\alpha\beta}^2$  is the quark charge squared and  $f_\pi$  is the weak  $\pi$  decay coupling constant. The latter is found, from the decay width for  $\pi \rightarrow \mu\nu$ , to have the value 93 MeV. This gives 7.6 eV for  $\Gamma_{\gamma\gamma}(\pi^0)$ , in good agreement with the experimental value quoted above.

Allowing for octet-singlet mixing as in (7), relations similar to (13) may be written for  $\eta, \eta'$ :

$$\Gamma_{\gamma\gamma}(\eta) = \frac{\alpha^2}{32\pi^3} \left[ \frac{S_8}{F_8} \cos\theta - \frac{S_1}{F_1} \sin\theta \right]^2 m_\eta^3 \quad (14a)$$

$$\Gamma_{\gamma\gamma}(\eta') = \frac{\alpha^2}{32\pi^3} \left[ \frac{S_8}{F_8} \sin\theta + \frac{S_1}{F_1} \cos\theta \right]^2 m_{\eta'}^3 \quad (14b)$$

$S_8, S_1$  are found, from the octet and singlet flavour wave functions:

$$|\eta_8\rangle = (1/\sqrt{6})(|u\bar{u}\rangle + |d\bar{d}\rangle - 2|s\bar{s}\rangle) \quad (15a)$$

$$|\eta_1\rangle = (1/\sqrt{3})(|u\bar{u}\rangle + |d\bar{d}\rangle + |s\bar{s}\rangle) \quad (15b)$$

to have the values presented in Table 2 for the FC and IC quark models.

Using Table 2 (14) may be rewritten as:

$$\Gamma_{\gamma\gamma}(\eta) = \frac{\alpha^2}{192\pi^3} \frac{1}{F_8^2} \left[ \cos\theta - 2\sqrt{2} \zeta r \sin\theta \right]^2 m_\eta^3 \quad (16a)$$

$$\Gamma_{\gamma\gamma}(\eta') = \frac{\alpha^2}{192\pi^3} \frac{1}{F_8^2} \left[ \sin\theta + 2\sqrt{2} \zeta r \cos\theta \right]^2 m_{\eta'}^3 \quad (16b)$$

$$r = F_8/F_1^*$$

\* Note that  $F_1, F_8$  in (16a,b) are the reciprocals of the amplitudes defined with an identical notation in [34].

where  $\zeta = 1, 2$  for the FC, IC quark models. Eqns (16) are derived from PCAC in just the same way as (13), but now large mass extrapolations from  $(q_1 + q_2)^2 = 0$  to  $m_{\eta, \eta'}^2$  are involved, and  $F_1, F_8$  are not simply related (as is  $f_\pi$ ) to other well known physical processes.

Since in (16)  $\zeta$  is always multiplied by the unknown ratio  $r$  a purely phenomenological analysis based on (16) cannot distinguish the FC ( $\zeta = 1$ ) from the IC ( $\zeta = 2$ ) models [3]. A test that evaluated  $r$  on the basis of the current algebra prediction for  $\Gamma_{\beta\gamma}(\eta)/\Gamma_{\gamma\gamma}(\eta)$  [3] is untrustworthy as the experimental ratio is considerably larger than the prediction for either the FC or IC models (16 as compared to upper limits of 7.1, 1.8 for the FC, IC models). Another test [4] based essentially on the agreement between the prediction given by (10a-c) for  $\Gamma_{\gamma\gamma}(\eta')$  and experiment is inconclusive, since, as discussed above, in this model the FC and IC models necessarily give identical predictions.

Further theoretical assumptions, or more detailed phenomenological input is needed before  $\Gamma_{\gamma\gamma}(\eta), \Gamma_{\gamma\gamma}(\eta')$  become sensitive to the value of  $\zeta$ . If the conditions:

$$\begin{aligned} F_\pi &= F_8 & \text{flavour SU(3) symmetry} \\ F_1 &= F_8 & \text{'nonet symmetry'} \end{aligned}$$

are imposed, then the measured value of  $\Gamma_{\gamma\gamma}(\eta')$  clearly favours fractional quark charges [2]. The nonet symmetry assumption is however inconsistent with the very strong breaking of this symmetry observed in the  $\pi^0, \eta, \eta'$  masses [3]. If it is assumed instead that  $r = 1/2$  (giving a large breaking of nonet symmetry, as observed for the masses of the states) the measured value of  $\Gamma_{\gamma\gamma}(\eta')$  gives  $\zeta = 2$  and so favours the IC model [3,34].

To make a meaningful test further 'dynamical' information is needed. In particular a quantitative estimate of SU(3) and nonet symmetry breaking effects must be made. The aim of the present work is to make such an estimate using a non-relativistic quarkonium model where SU(3) breaking is ac-

counted for by the difference in constituent masses of the strange and non-strange quarks, and nonet symmetry breaking by the interplay of large binding corrections and contributions to the potential from quarkonium annihilation into gluons for the isoscalar states.

#### 3.4 Quarkonium Annihilation Model

Applications of the quarkonium model to the light mesons have been made by many authors. Potential model calculations of the mass spectrum taking account of the strong hyperfine splitting effects in the S-wave states have been successful in explaining the observed mass spectrum [12,35,36], while other authors have considered quarkonium annihilation as a model for the  $2\gamma$  widths of light mesons [37-39].

The diagram for quarkonium annihilation into two photons is shown in Fig. 3b. The  $q\bar{q}$  are assumed to annihilate as free particles. The flux factor giving the interaction probability is proportional to  $|\psi(0)|^2$ ,  $|\partial\psi/\partial r|_{r=0}^2$  for  $0^-, 2^+$  states respectively.  $\psi(r)$  is the spatial wave function of the state.

The current algebra prediction using the triangle anomaly graphs (Fig. 3a) gives a result independent of the quark masses. In contrast the ratio between the constituent quark mass and the physical mass of the state plays an important role in the quarkonium annihilation model. Constituent quark masses of

$$m_u = m_d = m_{ns} = 336 \text{ MeV}/c^2 \quad m_s = 532 \text{ MeV}/c^2$$

as determined from baryon magnetic moments, and the masses of non-isoscalar light mesons [40] are used as fixed parameters in the present analysis.

For the pseudoscalar mesons  $\Gamma_{\gamma\gamma}$  is given by the expression:

$$\Gamma_{\gamma\gamma}(P) = \frac{4\pi\alpha_c^2}{3} \left[ \frac{\sum Q_i^2}{i} \frac{M_p}{(m_i^2 + M_p^2/4)} A_i^P f_i^{\text{QCD}} |\psi_i^P(0)|^2 \right]^2 \quad (17)$$

here:

$$\frac{1}{\sqrt{3}} Q_i^2 = \text{colour singlet projection of (quark charge)}^2, \text{ see (5)}$$

$M_p$  = mass of state P

$m_i$  = constituent quark mass ( $i = ns, s$ )

$A_i^P$  = amplitude of  $q_i\bar{q}_i$  ( $i = ns, s$ ) in the flavour wavefunction of P

$\psi_i^P(0)$  = spatial wavefunction at the origin

$$f_i^{\text{QCD}} = \text{first order QCD correction [41]} = \left[ 1 - \frac{3.38}{\pi} \alpha_s(m_i) \right]^{1/2}$$

where [39,42]

$$\alpha_s(M) = \alpha_s^0(M) \left[ 1 - \frac{(153-19 N_f)}{2\pi(33-2 N_f)} \alpha_s^0(M) \ln \left( \frac{M^2}{\Lambda^2} \right) \right]$$

$$\alpha_s^0(M) = \frac{12\pi}{(33-2N_f) \ln(M^2/\Lambda^2)}$$

giving:

$$\alpha_s(m_{ns}) = 0.42 \quad \alpha_s(m_s) = 0.31$$

for:

$$N_f = \text{number of quark flavours} = 4$$

$$\Lambda = 90 \text{ MeV}/c \quad [42]$$

$\alpha_s(m_{ns})$ ,  $\alpha_s(m_s)$  will be treated as fixed parameters with the above values in this analysis. The sensitivity of the results obtained to the value of  $\Lambda$  will be briefly discussed in Section 7.

Eqn (17) is the generalisation to several flavours of the classical parapositronium formula [43] when allowance is made for non-vanishing binding effects (i.e.  $M_p$ , in general =  $2 m_q$ ). For one flavour and  $M_p = 2 m_q$ , (17) reduces to the classical formula\* on neglecting the QCD correction.

The corresponding formula for the tensor mesons is [7]:

$$\Gamma_{YY}(T) = \frac{1152\pi\alpha^2}{5} \left[ \frac{\sum Q_i^2}{i\sqrt{3}} \frac{1-4(m_i/M_T)^2 + 28(m_i/M_T)^2 |1/2}{m_i^2} \frac{A_i^T}{A_i^T} \left| \frac{\partial\psi_i}{\partial r} \right|_{r=0} \right]^2 \quad (18)$$

Here no QCD correction is included.

The ratio of the wave functions (or the derivatives of the wave functions) at the origin for different quark flavours in a state with a fixed mass is given by non-relativistic potential theory [44]:

$$|\psi_{ns}(0)|/|\psi_s(0)| = (m_{ns}/m_s)^{3/4} \quad (19a)$$

$$|\partial\psi_{ns}/\partial r|_{r=0}/|\partial\psi_s/\partial r|_{r=0} = (m_{ns}/m_s)^{5/4} \quad (19b)$$

The mass scaling in (19a,b) corresponds to a logarithmic potential which gives a good fit to heavy quarkonium mass spectra and also describes well the masses of the first radially excited light meson states:  $\pi'$ ,  $\rho'$ ,  $\phi'$  (see the discussion in Section 5.7 below).

The question of the relevance of a non-relativistic theory to light meson systems should certainly be asked. A semi-quantitative discussion for the pseudoscalars will be given in Section 7. Here it is simply remarked that since, in all cases, only the ratio of radiative widths is considered when comparing theory and experiment relativistic

\*) Eqn (24) of [39] also gives the classical formula in the zero binding energy limit, but disagrees with (17). The origin of the discrepancy between these two formulae is unclear. Eqn (17) is however identical to (8) of [37] in the static non-relativistic limit  $p = 0$ , when the QCD correction is neglected.

corrections may be expected to largely cancel. This should be particularly true for the  $f$ ,  $A_2$  which have masses differing by only 4 % and wave functions which are found to contain almost purely non-strange quarks.

At the time of writing the status of explicit calculations of relativistic corrections is unclear. In [7] use of the non-relativistic formula (18) in conjunction with the wave functions found in [35] gives values for  $\Gamma_{YY}(A_2)$ ,  $\Gamma_{YY}(f)$  about 50 % larger than the experimental values. After including relativistic corrections the predictions fall about a factor of 3 below the experimental values. In contrast, for the  $f'$  the relativistically corrected value gives better agreement with the experiment. Relativistic corrections for pseudoscalar mesons are discussed below in Section 7.

The relationship between constituent and current quark masses has recently been discussed in the context of lattice gauge calculations by Samuel and Moriarty [45]. As in meson systems the  $q$  ( $\bar{q}$ ) is always effectively in the colour field of the  $\bar{q}$  ( $q$ ) it seems appropriate to use the constituent mass in the propagator factors of (17, 18). The current quark masses are relevant to free quarks [45] or to quarks that are effectively 'free' by asymptotic freedom because they participate in a process of scale  $Q \gg m_q$ . Neither of these possibilities are realised in light meson systems.

#### 4. LINEAR QUARKONIUM GLUONIUM MIXING MODEL

The analysis presented here uses a linear mass matrix to describe flavour mixing. This mixing, induced, in lowest order of QCD, by two gluon exchange (Fig. 4a), is directly analogous to that induced in the  $K^0-\bar{K}^0$  system by  $W^+W^-$  exchange (Fig. 4b). In the latter case a linear mass matrix has always been used. Neutrino oscillations are similarly described by a linear mass matrix.

The origin of the use of quadratic mass mixing formulae for the mesons was the approximate success of the quadratic Gell-Mann Okubo (GMO) mass formula:

$$M_K^2 = \frac{1}{4} (3 M_\pi^2 + M_\eta^2) \quad (20)$$

This was later given some theoretical justification in a bootstrap type model where the 'constituents' of the mesons are also mesons [46]. Since now, however, the masses of the pseudoscalar and vector mesons are most simply understood in terms of strong hyperfine splittings [40,47] resulting from 'chromomagnetic' terms in the potential, and from flavour mixing effects (for  $\eta, \eta'$ ) induced by gluonic intermediate states [40], the simple SU(3) symmetry breaking pattern underlying the GMO formula is in any case not expected to be valid [47]\*. From this point of view the success of the quadratic GMO formula (20) is fortuitous. The use of quadratic mass formulae can, however, be justified if the current algebra approach is used [48].

The philosophy adopted here follows closely that of [40] in seeing how far a simple model, based on constituent quarks and non-relativistic potential theory and including (as will be seen below) perturbative QCD estimates can go in describing the mass spectrum and transition amplitudes of light hadrons.

\*) This remarkable paper contains many of the successful predictions for the light hadron mass spectrum rederived, after the advent of QCD in [40].

It is more natural in such an approach, following [12,40], to use a linear mass matrix.

The model presented here is similar to that previously used to discuss quarkonium gluonium mixing by several authors [8-10] except that mass dependent SU(3) breaking corrections are included. Similar SU(3) breaking effects for pure quarkonium states using both quadratic [11,49] and linear [12] mass mixing formulae have been considered before in the literature.

The mass matrix is diagonalised using as basis  $|ns\rangle, |s\rangle, |G\rangle$  where:

$$\begin{aligned} |ns\rangle &= (\sqrt{2}) [ |u\bar{u}\rangle + |d\bar{d}\rangle ] \\ |s\rangle &= |s\bar{s}\rangle \\ |G\rangle &= |gg\rangle \end{aligned} \quad (21)$$

The state  $|G\rangle$  is supposed to be a pure gluonium bound state (glue ball). However, the mass mixing formalism would be identical if  $|G\rangle$  were any unitary singlet state (for example a radially excited pure quarkonium state). Such alternative explanations of the (1450) will be discussed in Section 5.6 below.

The mass matrix with the above basis is:

$$\mathcal{M} = \begin{bmatrix} M_{ns} + 2\alpha & & & & & \\ & \sqrt{2} Z_\alpha & & & & \\ & & M_s + Z_\alpha^2 & & & \\ & & & Z_\beta & & \\ & & & & Z_\beta & \\ & & & & & M_G \end{bmatrix} \quad (22)$$

The diagonal terms of the matrix are unmixed quarkonium or gluonium masses ( $M_{ns}, M_s, M_G$ ) or potential energy terms ( $2\alpha, Z_\alpha^2$ ) generated by annihilation into gluons.  $M_{ns}, M_s$  include hyperfine splitting corrections. The off diagonal terms ( $\sqrt{2}Z_\alpha, \sqrt{2}Z_\beta, Z_\beta$ ) correspond to flavour changing transition amplitudes. The interpretation of the five annihilation amplitudes in terms of the lowest order perturbative QCD diagrams is given in Fig. 5.

The parameter  $1-Z$  is a measure of the strength of  $SU(3)$  breaking effects. With massless gluons and the factorisation properties suggested by Figs. 4a,5  $Z$  can be estimated as:

$$Z(M_p) = \frac{\alpha_S(m_S) \left[ \frac{m_{ns}^2 + M_p^2/4}{m_S^2 + M_p^2/4} \right] \left( \frac{m_S}{m_{ns}} \right)^{3/4}}{\alpha_S(m_{ns}) \left[ \frac{m_{ns}^2 + M_p^2/4}{m_S^2 + M_p^2/4} \right] \left( \frac{m_S}{m_{ns}} \right)} \quad (23a)$$

$$\equiv Z_p \frac{\left[ \frac{m_{ns}^2 + M_p^2/4}{m_S^2 + M_p^2/4} \right]}{\left[ \frac{m_{ns}^2 + M_p^2/4}{m_S^2 + M_p^2/4} \right]} \quad (\text{pseudoscalars})$$

$$Z(M_T) = \frac{\alpha_S(m_S) \left[ \frac{1-4(m_S/M_T)^2}{1-4(m_S/M_T)^2 + 28(m_S/M_T)^2} \right]^{1/2} \left( \frac{m_{ns}}{m_S} \right)^2 \left( \frac{m_S}{m_{ns}} \right)^{5/4}}{\alpha_S(m_{ns}) \left[ \frac{1-4(m_S/M_T)^2}{1-4(m_S/M_T)^2 + 28(m_S/M_T)^2} \right]^{1/2} \left( \frac{m_{ns}}{m_S} \right)^2 \left( \frac{m_S}{m_{ns}} \right)^{5/4}} \quad (23b)$$

$$\equiv Z_T \frac{\left[ \frac{1-4(m_S/M_T)^2}{1-4(m_S/M_T)^2 + 28(m_S/M_T)^2} \right]^{1/2}}{\left[ \frac{1-4(m_S/M_T)^2}{1-4(m_S/M_T)^2 + 28(m_S/M_T)^2} \right]^{1/2}} \quad (\text{tensors})$$

The lowest order QCD predictions for  $Z(M_p)$ ,  $Z_p$ ,  $Z(M_T)$ ,  $Z_T$  are presented in Table 3. It can be seen that, particularly for the pseudoscalars, the expected  $SU(3)$  breaking effects are large and mass dependent.

The mass dependence of  $M$  implies that its eigenstates are not, in general, orthogonal. Writing an eigenstate  $|j\rangle$  as\*:

$$|j\rangle = x_j |ns\rangle + y_j |s\rangle + z_j |G\rangle \quad (24)$$

The ratio  $y_j/x_j$  is found to depend only on the mass eigenvalue  $M_j$ ,  $M_{ns}$ ,  $M_S$  and  $Z(M_j)$

$$y_j/x_j = (1/\sqrt{2}) Z(M_j) \frac{(M_j - M_{ns})}{(M_j - M_S)} \quad (25)$$

i. e. it is independent of the strength of the mixing amplitudes  $\alpha$ ,  $\beta$ .

Of the six parameters necessary to completely define  $M$  three may be determined from the physical masses of the states using the eigenvalue

\*) Here the notation of [9] is followed.

equations, while  $M_{ns}$  is given by the mass of the isospin one non-strange state ( $\pi^0$ ,  $A_2$  for  $0^+$ ,  $2^+$ ). This leaves two free parameters, which are chosen to be  $Z_p$  or  $Z_T$  and  $M_S$ . In the phenomenological fits presented below these parameters are varied so as to minimise the overall  $\chi^2$ . The fit values of these parameters may then be compared with the perturbative QCD expectations of Table 3 for  $Z_p$ ,  $Z_T$  or quark model expectations (including hyperfine splitting corrections [40,47] in the case of the pseudoscalars) for  $M_S$ .

A further constraint is provided by the measured ratio:

$$\Gamma_{\eta' \gamma}(J/\psi) / \Gamma_{\eta \gamma}(J/\psi)$$

Noting that, quite generally, factorisation is expected between the transition amplitude for  $J/\psi \rightarrow f\bar{f}\gamma$  ( $f = ns, s, g$ ) and the corresponding element of the mass matrix  $\mathcal{M}$  (22) then [31]:

$$\Gamma_{\eta' \gamma}(J/\psi) / \Gamma_{\eta \gamma}(J/\psi) = \frac{\{ [M_{\eta\eta'}^2 - M_{\eta\eta}^2]^2 \{ \alpha(x_{\eta'} + Z_{Y_{\eta'}}) + \beta z_{\eta'} \}^2 \}}{\{ \dots \}} = 4.2 \pm 0.7 \quad (26)$$

The factorisation is illustrated in Fig. 6, where as an example, the corresponding lowest order QCD diagrams are shown. The factorisation property is expected, however, to be of more general validity than the specific QCD diagrams shown in Fig. 6.

### 5.3 Constraint from Strong Processes Using the OZI Rule

As pointed out by Okubo and Jagannathan [51] use of the OZI (Okubo-Zweig-Iizuka [52]) rule in hadronic processes can provide information on the flavour content of the  $\eta$  and  $\eta'$  mesons. Here the ratios:

$$\frac{\Gamma_{\eta\pi}(A_2) / \Gamma_{\eta\pi}(A_2)}{\sigma_f(\pi^+ p \rightarrow \eta' n) / \sigma_f(\pi^+ p \rightarrow \eta n)}$$

(where  $\sigma_f$  denotes the forward scattering cross section) are chosen.

To calculate  $\Gamma_{pp}(\pi)$  a simple model [13] based on additive duality amplitudes, with a correction factor to account for phase space and the D-wave angular momentum barrier, is used. Unlike in [13] however SU(3) breaking is allowed for by assuming a constant ratio (see Fig. 7a):

$$\frac{A(q\bar{q} \rightarrow (q\bar{s})(\bar{q}s))}{A(q\bar{q} \rightarrow (q\bar{n}s)(\bar{q}ns))} = \xi$$

## 5. PSEUDOSCALAR MESON ANALYSIS

### 5.1 Analysis Method

The procedure adopted to test the IC and FC models for the pseudoscalar mesons is to first make a fit where the flavour amplitudes  $x, y, z$  for  $\eta, \eta'$  are determined by using measured  $1\gamma$  and strong decay transition widths that are independent of the quark charges. The mixing matrix (22) is used with fixed masses 548, 958, 1450 MeV/c<sup>2</sup> [31,50] for the  $\eta, \eta', 1, M_S$  and  $Z_P$  are varied so as to minimise the  $\chi^2$  of a fit to the experimental data. Since  $M_{ns} = M_{\eta 0}$  the physical masses determine, via the eigenvalue equations all six parameters needed to specify  $\mathcal{M}$ .

The quark charges are then tested by comparing the predictions given by (17) for the IC and FC models with the experimental value of  $\Gamma_{\eta\gamma}(\eta')$ . For this an estimate of  $\psi(0)$  for the  $\eta'$  is needed. This is obtained from the experimental value of  $\Gamma_{e^+e^-}(\omega)$  and (10a) on the hypothesis that  $\psi(0)$  is spin independent for a given mass and flavour composition.

Predictions are also given for various transition rates and branching ratios involving the  $\psi(1450)$ . These provide further tests of the overall consistency of the model.

### 5.2 Constraints from the Transitions $P(V) \rightarrow V(P)\gamma$

For transitions between the light pseudoscalar and vector mesons, constraints previously given by Rosner [9] are used. Eqns (10b) and the measured ratios:

$$\Gamma_{\eta\gamma}(\rho) / \Gamma_{\pi\gamma}(\omega), \quad \Gamma_{\rho\gamma}(\eta') / \Gamma_{\pi\gamma}(\omega), \quad \Gamma_{\eta\gamma}(\phi) / \Gamma_{\pi\gamma}(\omega)$$

yield the constraints on  $x_{\eta}, x_{\eta'}, y_{\eta}, y_{\eta'}$  presented in Table 4. It is assumed that  $\mu_i = I_i = 1$  in (10b), but SU(3) breaking resulting from  $m_{ns} \neq m_s$  is included.

$\xi$  is found to be  $0.89 \pm 0.06$  from a fit to the measured values of  $\Gamma_{\pi\pi}(f, f')$   $\Gamma_{KK}(f, f')$  described in Section 6.2 below.

The model gives [31]:

$$\Gamma_{\eta\pi}(A_2)/\Gamma_{KK}(A_2) = \frac{2}{\xi^2} \left( \frac{P_\eta}{P_K} \right)^5 (x_\eta + v y_\eta)^2 = 3.0 \pm 0.4 \quad (27)$$

Here  $v$  allows for a possible violation of the OZI rule by a ' $Z\alpha'$ ' (see Fig. 5) type amplitude.

The duality diagram of Fig. 7b and the experimental measurement [53] give the constraint:

$$\left| \frac{x_{\eta'} + v y_{\eta'}}{x_\eta + v y_\eta} \right| = 0.74 \pm 0.04 \quad (28)$$

where the OZI rule violating amplitude is assumed to be process independent. To simplify the fitting procedure, and in view of the small experimental error in (28), only (27) is used in the fit, (28) being used to eliminate the parameter  $v$  from (27) neglecting the experimental error in (28). In fact as shown below, the best fit value of  $v$  is consistent with zero.

#### 5.4 Results of the Fit to the Mass Matrix

The best fit to the 5 constraints (4 from  $1\gamma$  transitions, 1 from strong decays) which is summarised in Table 4, has a  $\chi^2$  of 1.85 for 3 degrees of freedom. The fitted parameters of the mixing matrix  $\mathcal{M}$  are presented in Table 5, while the eigenvectors corresponding to the physical  $\eta, \eta', \iota$  states are shown in Table 6. Errors are quoted at the  $\chi^2_{\text{MIN}} + 1$  level.

The following comments may be made on the results of the fit:

i) The mass  $M_S$  of the pure  $s\bar{s}$  quarkonium state may be compared with the expectation from the hyperfine mass splitting formula [40,47] (see Section 5.7 below). A simplified version of the formula [9] gives:

$$M_S = M_\psi - \frac{(M_{K^*} - M_K)^2}{M_\rho - M_\pi} = 0.77 \text{ GeV}/c^2$$

which is 15 % larger than the fitted value. The more refined analysis of Section 5.7 gives  $M_S = 0.644 \text{ GeV}/c^2$ , only 4 % less than the fitted value.

ii) The unmixed pseudoscalar glueball mass is found to be  $1.22 \pm 0.05 \text{ GeV}/c^2$ . This is at the lower limit of the range of masses found in a lattice gauge calculation [54]:

$$M_G = \begin{matrix} 1.42 & +0.24 \\ & -0.17 \end{matrix}$$

and somewhat lower than predictions of 1.3 - 1.4  $\text{GeV}/c^2$  using Bag [55] or Potential [56] models, respectively. The interpretation of the state  $|G\rangle$  as a radially excited pure quarkonium state [57] will be discussed below in Section 5.7.

iii) As found previously [40,58,59] the annihilation term  $\alpha$  is large (0.36  $\text{GeV}/c^2$ ) as compared to the pion mass. This explains, even in the absence of direct mixing with the heavy state  $|G\rangle$ , the large deviation from ideal mixing observed in the  $\pi^0, \eta, \eta'$  masses. More unexpected perhaps is the somewhat smaller value of  $\beta$  (0.153  $\text{GeV}/c^2$ ), as colour charge factors favour  $ggg$  over  $q\bar{q}g$  couplings by a factor 9/4 (see Fig. 5). The suppression is, however, naturally explained in the naive gluonium model as the wave function at the origin vanishes for pseudoscalar gluonium.

It should be remarked that in the present model the transitions  $J/\psi \rightarrow P\gamma$  ( $P = \eta, \eta', \iota$ ) are not, as is commonly assumed, dominated by the glueball component in the flavour wave functions. In fact the ratio of the 'quarkonium' transition amplitude  $\alpha(x + Zy)$  to the 'gluonium' amplitude  $\beta z$  (see Fig. 6) is 5.6, 3.3 for  $\eta, \eta'$ , respectively. The SU(3) breaking parameter  $Z_p$  has a dramatic effect on the ratio of transition rates in (26). Setting  $Z_p = 1$  gives:



$$\Gamma_{\eta', \gamma}(J/\psi) / \Gamma_{\eta', \gamma}(J/\psi) = 36$$

illustrating the importance of including SU(3) breaking to obtain the good overall fit shown in Table 4.

- iv) The SU(3) breaking parameter  $Z_p = 0.89 \pm 0.03$  is some 14 % smaller than the lowest order QCD estimate of 1.04 (see Table 3). Considering the large experimental uncertainty in the value of  $\alpha_s$  this agreement is quite satisfactory. The sensitivity of  $Z_p$  to the scale parameter  $\Lambda$  of QCD is briefly discussed below in Section 7.
- v) The value of the OZI rule violating parameter calculated from the fitted values of  $x_{\eta, \eta'}, y_{\eta, \eta'}$  and (28) is:
- $$v = -0.01 \pm 0.03$$
- consistent with zero, justifying the use of the simple duality amplitudes shown in Fig. 7a for processes involving  $\eta, \eta'$ .
- vi) The flavour wave functions presented in Table 6 indicate significant admixtures of the state  $|G\rangle$  in all three physical states. All states contain roughly equal amplitudes for strange and non-strange quarks, while the  $\eta'$  and  $\eta$  each have a  $|G\rangle$  amplitude of 0.6-0.7, but with different signs.

Recently the decays:

$$J/\psi \rightarrow PV \quad P = \pi, K, \eta, \eta'; \quad V = \rho, \omega, \phi, K^*$$

have been measured in the MARK III detector at SPEAR. A preliminary analysis using only the simplest (singly disconnected) OZI rule violating diagrams has reached a similar conclusion to the present paper on the necessity for a gluonium component in the  $\eta'$  [60,61]. It is found that [61]:

$$\begin{aligned} x_{\eta}^2 + y_{\eta}^2 &= 1.1 \pm 0.1 \\ x_{\eta'}^2 + y_{\eta'}^2 &= 0.65 \pm 0.12 \end{aligned}$$

which may be compared with:

$$\begin{aligned} x_{\eta}^2 + y_{\eta}^2 &= 0.98 \pm 0.04 \\ x_{\eta'}^2 + y_{\eta'}^2 &= 0.62 \pm 0.06 \end{aligned}$$

from Table 6. In more detail, the fitted values of  $x_{\eta, \eta'}, y_{\eta, \eta'}$  in the MARK III analysis are in agreement with the values in Table 6 except for  $|x_{\eta'}|$  where a value of  $0.34 \pm 0.04$  is quoted, inconsistent with the constraint given by  $\Gamma_{\rho\gamma}(\eta') / \Gamma_{\rho\gamma}(\omega)$  shown in Table 4. A possible resolution of this discrepancy may be the inclusion of doubly disconnected OZI rule violating diagrams in the MARK III analysis. In any case two completely independent phenomenological analyses each indicate an amplitude of  $\approx 60\%$  'non ground state quarkonium' in the  $\eta'$  flavour wave function\*.

### 5.5 Tests of the Quark Charges

Before the quarkonium annihilation formula (17) can be used to test the quark charge factors  $Q_i^2$  for the FC or IC model (Table 1) a further phenomenological input is needed to estimate the spatial wave function at the origin of the state in question. Following previous authors [37,38,62] the ansatz is made that the wave function at the origin has a power law dependence on the mass of the state:

$$|\psi_{ns}^P(0)|^2 \sim M_P^{\nu} \quad (29)$$

For a given quark charge assignment the exponent  $\nu$  is determined from (17), the flavour amplitudes in Table 6 and the experimental ratio

\*) Strictly speaking the phenomenological analyses demonstrate only that there is an 'inert' portion of the flavour wave-function as probed by photon pairs or by quark line diagrams. Other explanations, e. g. a radially excited quarkonium admixtures which are 'inert' because of a much smaller wave-function at the origin, should also be considered a priori. See the discussion in Section 5.7.

$\Gamma_{\gamma\gamma}(\eta)/\Gamma_{\gamma\gamma}(\eta)$ . The actual value of the wave function is estimated by assuming that, for a fixed mass, it is independent of the spin state of the quarks. A similar assumption was made in [38]. Then:

$$\left| \psi_{\eta^0}(\omega) \right| = \left| \psi_{\eta^0}(\omega) \right| \quad (30)$$

where  $M_{\eta^0} = M_{\eta^0}$ .

In this way the wave function at the origin for the  $\eta^0$  can be determined from the measured decay width of  $\omega \rightarrow e^+ e^-$  [31]:

$$\Gamma_{e^+e^-}(\omega) = \frac{8\pi\alpha^2}{9 M_\omega^2} \left[ 1 - \frac{5.33 \alpha_S(M_\omega)}{\pi} \right] \left| \psi_{\eta^0}(\omega) \right|^2 \quad (31)$$

$$= 0.71 \pm 0.07 \text{ keV}$$

$\omega - \phi$  mixing is neglected, but as in (17) the first order QCD correction [41], is taken into account. With  $\Lambda = 90 \text{ MeV}/c$ ,  $\alpha_S(M_\omega) = 0.26$ . The extrapolation of  $\psi(0)$  from  $M_\omega$  to  $M_{\eta^0}$  ( $P = \pi^0, \eta^0, \eta^0$ ) is done using the exponent  $n$  determined by (29).

The experimental situation of  $\Gamma_{\gamma\gamma}(\eta^0, \eta)$  is summarised in Table 7. The six independent measurements of  $\Gamma_{\gamma\gamma}(\eta^0, \eta)$  are consistent with their weighted average ( $\chi^2 = 5.0, 5 \text{ D.F.}$ ) unlike the four measurements of  $\Gamma_{\gamma\gamma}(\eta)$  ( $\chi^2 = 29, 3 \text{ D.F.}$ ). For the  $\eta$  the two (self consistent) recent measurements of Crystal ball and JADE [1] are considered separately from the Primakoff values [69,70].

The average values of  $\Gamma_{\gamma\gamma}(\eta^0, \eta)$  from Table 7 and (29) yield:

$$\begin{aligned} n &= 2.6 \pm 0.3 & \text{FC} \\ &= 1.02 \pm 0.30 & \text{IC} \\ &= -0.37 & \text{IC} \end{aligned}$$

Eqns (17,29-31) then predict the values of  $\Gamma_{\gamma\gamma}(\pi^0, \eta^0, \eta)$  presented in the first two columns of Table 8 for the FC, IC models respectively. The IC model is excluded by  $\Gamma_{\gamma\gamma}(\eta^0)$ , and FC is strongly favoured by  $\Gamma_{\gamma\gamma}(\pi^0)$ .

For the  $\pi^0$  (17) is written:

$$\Gamma_{\gamma\gamma}(\pi^0) = \frac{2\pi\alpha^2}{3} \frac{M_{\pi^0}^2}{(m_{\eta^0}^2 + M_{\pi^0}^2/4)^2} \left[ 1 - \frac{3.38}{\pi} \alpha_S(m_{\eta^0}) \right] \left| \psi_{\eta^0}(\omega) \right|^2 \quad (32)$$

The value of  $\Gamma_{\gamma\gamma}(\pi^0)$  for a given  $\psi(0)$  is the same in the FC and IC models, but because of the dependence of  $|\psi(0)|^2$  on  $n$ , the overall consistency of the model is still checked by the measured value of  $\Gamma_{\gamma\gamma}(\pi^0)$ .

Since:

$$\frac{m_{\pi^0}^2}{m_{\eta^0}^2} \gg \frac{m_{\pi^0}^2}{4}$$

$\Gamma_{\gamma\gamma}(\pi^0)$  is effectively  $\sim 1/m_{\eta^0}^4$  and so is very sensitive to the assumed constituent quark mass. The effect of changing  $m_{\eta^0}$  from the standard value of  $336 \text{ MeV}/c^2$  to  $300 \text{ MeV}/c^2$  is shown in Table 8.

Table 8 also presents the FC model values of  $\Gamma_{\gamma\gamma}(\pi^0, \eta^0, \eta)$  using:

- i)  $\Gamma_{\gamma\gamma}(\eta)$  from [73] DESY Primakoff experiment
- ii)  $\Gamma_{\gamma\gamma}(\eta)$  from [74] Cornell Primakoff experiment
- iii) (17), (31) without the QCD correction
- iv) pure quarkonium wave functions ( $\theta = -12^\circ$ ) for  $\eta, \eta^0$ .

It can be seen that  $\Gamma_{\gamma\gamma}(\pi^0)$  somewhat disfavours both Primakoff measurements, and favours the QCD corrected formulae. The very strong dependence of  $\Gamma_{\gamma\gamma}(\pi^0)$  on  $m_{\eta^0}$  should not however be forgotten - a small change in  $m_{\eta^0}$  can render both (ii) and (iii) compatible with experiment within the large errors. The 'no gluonium' case (iv) gives a predicted value of  $\Gamma_{\gamma\gamma}(\eta^0)$  which lies  $2.3\sigma$  above experiment. This is additional suggestive evidence, independent of that presented above, of the necessity, within the present model, for an explicit gluonium component in the  $\eta^0$  wave function.

As stated in Section 2 the IC model is only excluded by the results presented in Table 8 in the limit  $m_g^2 \gg \langle q^2 \rangle$  where  $m_g$  is the effective gluon mass in the IC theory and  $\langle q^2 \rangle$  is the average value of  $q^2$  of the virtual photons contributing to the experimental determination of  $\Gamma_{\gamma\gamma}$ . If the additional assumption is made in the IC model that the radiative width is dominated by quarkonium annihilation (i. e. charged gluonium annihilation

is neglected) then the measured value of  $\Gamma_{\gamma\gamma}(n')$  can provide an upper limit on the parameter  $m_g$  of the IC model. The neglect of gluonium annihilation may be justified by the vanishing of  $\psi(0)$  in the pseudoscalar  $g^+g^- \rightarrow \gamma\gamma$  amplitude.

Eqns (5,17) and Table 6 then give for the IC model:

$$\Gamma_{\gamma\gamma}(n')_{IC} = \Gamma_{\gamma\gamma}(n')_{FC} \left[ 1 + \frac{1.11 m_g^4}{(m_g^2 + q_1^2)(m_g^2 + q_2^2)} \right]^2 \quad (33)$$

where  $\langle \rangle$  denotes an average over the distribution of  $q_1^2, q_2^2$  for the experimental measurement.

In experiments detecting  $n'$  production in  $e^+e^-$  collisions [64-68] a stringent cut of  $\lesssim 200$  MeV/c is typically made on the transverse momentum of the  $n'$  ( $p_{\perp}^{n'}$ ) relative to the  $e^+e^-$  beams. This constrains  $q_1^2, q_2^2$  to low values and reduces the upper limit on  $m_g^2$ .

Performing the average in (33) using the exact "luminosity function" for transverse photons [71] gives the curves of  $\Gamma_{\gamma\gamma}(n')$   $\text{Exp}/\Gamma_{\gamma\gamma}(n')$  IC as a function of  $m_g$  shown in Fig. 8. Curves are drawn for  $p_{\perp}^{n'} \leq 0.1, 0.2$  GeV/c, and without a  $p_{\perp}^{n'}$  cut. In all cases the condition  $|y^{n'}| < 0.5$  (where  $y^{n'}$  is the lab. rapidity of the  $n'$ ) is imposed. This last cut is to allow for the limited angular acceptance of the detectors used in [64-68]. It corresponds to an angular cut  $\geq 30^\circ$  for the decay products of the  $n'$ .  $m_g$  is limited to  $\leq 0.6$  MeV/c<sup>2</sup> for  $p_{\perp}^{n'} \leq 0.1$  GeV/c<sup>2</sup>, and to  $\leq 1.0$  MeV/c<sup>2</sup> in the absence of a  $p_{\perp}^{n'}$  cut, by the experimental value of  $\Gamma_{\gamma\gamma}(n')$  given in Table 7. Both limits are quoted at the 95 % confidence level.

### 5.6 Predictions for $\iota(1450)$

Some predictions for radiative decay widths and branching ratios of the  $\iota(1450)$  are compared, in Table 9, with the existing experimental data. The prediction for  $\text{BR}(J/\psi \rightarrow \iota\gamma)$  uses the measured  $\text{BR}(J/\psi \rightarrow \eta\gamma)$  [31] and (26) with the replacement  $n' \rightarrow \iota$ . The  $1\gamma$  transition widths  $\Gamma_{\rho\gamma}(\iota), \Gamma_{\omega\gamma}(\iota), \Gamma_{\phi\gamma}(\iota)$  are given by (10b) and the flavour amplitudes in Table 6. All the predic-

tions are consistent with the present experimental limits.

Of particular interest is  $\text{BR}(J/\psi \rightarrow \iota\gamma)$   $\text{BR}(\iota \rightarrow \rho\gamma)$  which checks (admittedly within a large error of  $\pm 40$  %) the predictions for  $\text{BR}(J/\psi \rightarrow \iota\gamma)$  and  $\Gamma_{\rho\gamma}(\iota)$ . The latter is sensitive to the large non-strange quarkonium component in the  $\iota$ . Crucial tests of the model are provided by  $\Gamma_{\gamma\gamma}(\iota)$   $\text{BR}(\iota \rightarrow \text{KK}\pi)$  and  $\text{BR}(J/\psi \rightarrow \iota\gamma)$   $\text{BR}(\iota \rightarrow \phi\gamma)$ , the latter checking the strange quarkonium component of the  $\iota$ .

It is interesting to note that the predicted values of  $\Gamma_{\rho\gamma}(\iota), \Gamma_{\omega\gamma}(\iota), \Gamma_{\phi\gamma}(\iota)$  when inserted in the Van-Royen Weisskopf formula (10c) give  $\Gamma_{\gamma\gamma}(\iota) = 9.9$  keV, in good agreement with the quarkonium annihilation prediction of  $10 \pm 3$  keV.

A further important test of the model is the cross section ratio:

$$\sigma_f(\pi^+p \rightarrow \iota n) / \sigma_f(\pi^+p \rightarrow n'n)$$

(see section 5.3 above). As the non-strange amplitudes in the  $n'$  and  $\iota$  are predicted to be almost equal, the above cross section ratio should be close to one at high energies, where phase space corrections are small.

### 5.7 Radially Excited Quarkonium Interpretation of $\iota(1450)$

Several authors [57,72-74] have suggested that the  $\iota(1450)$  may be interpreted as a radially excited quarkonium state. A brief discussion of this possibility is now given. Mixing amplitudes are derived from the ground state mass matrix. General results of non-relativistic potential theory are then used to connect the ground and first excited states.

The best established radial excitation states experimentally are the vector mesons  $\rho'(1600)$  and  $\phi'(1680)$  [31]. The strong hyperfine mass splitting formula [40,47] is used to relate the masses of the pseudoscalar and vector states:

$$M(^3S_1) - M(^1S_0) = 4 \Delta_p^i = \frac{32\pi\alpha_s(m_i)}{9 m_i^2} \left| \int \psi_p(0) \psi_p'(0) \right|^2 \quad (34)$$

Here  $i = ns$ ,  $s$  denotes flavour and  $p = 1, 2$  for the ground and first excited states, respectively. Spectroscopic notation is used to denote the vector and pseudoscalar states. In (34)  $\psi(0)$  is assumed to be the same for the  ${}^3S_1$  and  ${}^1S_0$   $q\bar{q}$  states.

For a potential of the form:

$$V(r) = \lambda r^\nu \quad (35)$$

the ratio of the wave functions at the origin for the S-wave ground and first excited states,  $\psi_1(0)$ ,  $\psi_2(0)$ , respectively, is given by [44]:

$$\left| \frac{\psi_2(0)}{\psi_1(0)} \right|^2 = \left[ \frac{2-\gamma(\nu)}{1-\gamma(\nu)} \right] \frac{\nu-2}{2+\nu} \quad (36)$$

where  $\gamma(\nu) = \frac{1}{2} \left( \frac{1+\nu}{2+\nu} \right)$  and  $-2 < \nu \leq 0$ .

If both the  ${}^3S_1$  and  ${}^1S_0$  wave functions obey (36), then using the ground state splitting  $m_\rho - m_\pi$  and the physical  $\rho'$  mass, (34) gives predictions for  $M_\pi$  as a function of  $\nu$ . The results for  $\nu = 0, -1/2, -1$  are shown in Table 10. Choosing  $\nu = 0^*$  gives a value of  $m_\pi$  in good agreement with the experimental mass of  $1300 \pm 100$  MeV/c<sup>2</sup>.

The strong hyperfine operator:

$$O_{HF} = \frac{32\pi\alpha_s}{9 m_i m_j} \delta(r) S_i \cdot S_j \quad (37)$$

will also mix ground and radially excited states of a given spin parity and flavour content.  $S_i, S_j$  are the spins of the quarks of mass  $m_i, m_j$  separated by distance  $r$ . The spin vector product takes the values:

$$\begin{aligned} S_i \cdot S_j &= 1/4 & ({}^3S_1) \\ &= -3/4 & ({}^1S_0) \end{aligned}$$

\* This corresponds to a logarithmic potential which has been shown [75] to give a good description of the masses of heavy ( $c\bar{c}$ ,  $b\bar{b}$ ) quarkonium states.

which yield (34) for the vector-pseudoscalar mass splitting.

For the isospin zero pseudoscalar states the operator  $O_G$  describing quarkonium annihilation into multigluon states (see Fig. 5) will contribute to both flavour diagonal ( $\alpha$ ) and flavour non-diagonal ( $Z\alpha$ ) mixing.  $O_{HF}$  on the other hand gives only flavour diagonal interactions. Because of the opposite signs of  $O_{HF}$ ,  $O_G$  radial mixing is expected to be weaker for isospin zero, than for isospin one states where only  $O_{HF}$  contributes.

To estimate the annihilation amplitude for a pure quarkonium ( ${}^1S_0$ ) ground state a mass matrix in the basis  $\psi_1^{ns}, \psi_1^s$  is used:

$$\begin{pmatrix} M_{1ns}^0 - 3\Delta_1^{ns} + 2\alpha & \sqrt{2}Z\alpha \\ \sqrt{2}Z\alpha & M_{1s}^0 - 3\Delta_1^s + Z^2\alpha \end{pmatrix} \quad (38)$$

The hyperfine mass splittings  $\Delta_1^{ns}, \Delta_1^s$  are given by the  $\rho - \pi$  mass difference and (34):

$$\Delta_1^{ns} = (M_\rho - M_\pi)/4 \quad (39a)$$

$$\Delta_1^s = \frac{\alpha_s(m_s)}{\alpha_s(m_{ns})} \frac{|\psi_s(0)|^2}{|\psi_{ns}(0)|^2} \frac{m_{ns}^2}{m_s^2} \quad (39b)$$

Taking the values of the quark masses and  $\alpha_s$  from Section 3.4 and using (19a):

$$\Delta_1^s = 94 \text{ MeV}/c^2.$$

Neglecting annihilation mixing for the vector state, (34) then gives:

$$M_{1s}^0 = M_\phi - \Delta_1^s = 926 \text{ MeV}/c^2$$

The value of  $M_s = M_{1s}^0 - 3\Delta_1^s$  is found to be  $644 \text{ MeV}/c^2$  close to the fitted value, including gluonium mixing, of  $670 \pm 10 \text{ MeV}/c^2$  (Table 5). With

$$M_{1ns}^0 - 3\Delta_1^{ns} = M_\pi = 135 \text{ MeV}/c^2$$

and eigenvalues corresponding to  $\eta(548)$ ,  $\eta'(958)$  for (38) the eigenvalue equations may be solved for  $\alpha$  and  $Z^*$ . This gives:

$$\alpha = 344 \text{ MeV}/c^2, \quad Z = 0.421$$

The value of  $\alpha$  agrees well with that found including gluonium mixing,  $\alpha = 360 \pm 18 \text{ MeV}/c^2$ , but  $Z$  is significantly (26 %) lower than the mean of  $Z(M_\eta)$ ,  $Z(M_\eta)$  as given the fitted value of  $Z_p$  in Table 5 and (23a). So the magnitude of the SU(3) breaking agrees better with the perturbative QCD estimate when gluonium mixing is included, than for the pure quarkonium case.

The transition amplitudes  $\alpha$ ,  $Z\alpha$ ,  $Z^2\alpha$  are proportional to the wave function at the origin. Eqn (36) may be written as:

$$\left| \psi_2(0) \right| = Y \left| \psi_1(0) \right| \quad (40)$$

where, for the favoured value  $\nu = 0$  of the exponent in (35),  $Y = 0.66$ . Using (40) the mass matrix (22) may be generalised to include the first radially excited quarkonium states. The matrix in the basis  $\psi_1^{ns}$ ,  $\psi_2^{ns}$ ,  $\psi_1^s$ ,  $\psi_2^s$ ,  $G$  is given in Table 11. The unperturbed quarkonium mass terms are given by the relations:

$$\begin{aligned} M_{1ns}^0 &= M_\pi + 3\Delta_1^{ns} = 0.606 \text{ GeV}/c^2 \\ M_{2ns}^0 &= M_{\rho'} - \Delta_1^{ns} \quad Y^2 = 1.532 \text{ GeV}/c^2 \\ M_{1s}^0 &= M_\phi - \Delta_1^s = 0.926 \text{ GeV}/c^2 \\ M_{2s}^0 &= M_\phi - \Delta_1^{s2} = 1.639 \text{ GeV}/c^2 \end{aligned} \quad (41)$$

The SU(3) breaking parameters are estimated from (23a) to be:

\* ) Here assumed to be mass independent.

$$Z_{11} = 0.53 \quad Z_{12} = 0.65 \quad Z_{22} = 0.72 \quad (42)$$

The different values account for the different mean masses appropriate to various mixing amplitudes.

If gluonium mixing is absent the eigenstates are found by diagonalising the matrix formed by the first 4 rows and columns of Table 11. With  $\alpha = \text{MeV}/c^2$ ,  $Y = 0.66$  and other parameters as in (41), (42) the eigenvectors and eigenvalues (in  $\text{MeV}/c^2$ ) are:

$$\begin{aligned} \eta_1(520) &= 0.709|\psi_1^{ns}\rangle + 0.068|\psi_1^{ns}\rangle - 0.673|\psi_1^s\rangle + 0.202|\psi_2^s\rangle > \\ \eta_1'(978) &= 0.659|\psi_1^{ns}\rangle - 0.339|\psi_1^{ns}\rangle + 0.670|\psi_1^s\rangle - 0.035|\psi_2^s\rangle > \\ \eta_2(1515) &= -0.016|\psi_1^{ns}\rangle + 0.584|\psi_2^{ns}\rangle + 0.272|\psi_1^s\rangle - 0.765|\psi_2^s\rangle > \\ \eta_2'(1830) &= 0.252|\psi_1^{ns}\rangle + 0.734|\psi_2^{ns}\rangle + 0.156|\psi_1^s\rangle + 0.611|\psi_2^s\rangle > \end{aligned} \quad (43)$$

To compare this solution with the pure ground state results of Table 6 it is useful to define 'effective' flavour amplitudes by the relations:

$$\begin{aligned} x_{ef} &= x_1 + Yx_2 \\ y_{ef} &= y_1 + Yy_2 \end{aligned} \quad (44)$$

Here the subscripts 1, 2 on  $x$ ,  $y$  refer to the ground and first excited states, respectively. To correct for the effect of radial excitations in transition amplitudes,  $x$ ,  $y$  in the pure ground state case are replaced by  $x_{ef}$ ,  $y_{ef}$ : The phase convention used here is that  $\psi_1^i(0)$ ,  $\psi_2^i(0)$  have the same sign.

The values of  $x$ ,  $y$  from Table 6 are compared with  $x_{ef}$ ,  $y_{ef}$  from (43, 44) in Table 12. For  $(\eta, \eta_1)$  or  $(\eta', \eta_1')$  the absolute values agree within 15 % or better, and the relative signs are the same.

Is it possible that the physical  $\psi(1450)$  can be identified with the state  $\eta_2(1515)$  of (43)? From (26) with the replacements  $\eta' \rightarrow \eta_2$ ,  $\beta = 0$  it is found that

$$\text{BR}(J/\psi \rightarrow \eta_2(1515)\gamma) = 2.6 \times 10^{-4}$$

as compared to the experimental branching ratio [61]:

$$\text{BR}(J/\psi \rightarrow \psi(1450)\gamma) > 4.9 \times 10^{-3}$$

The low predicted branching ratio results from the relative negative sign of  $x_{\text{ef}}, y_{\text{ef}}$  in  $\eta_2$  and is relatively insensitive to their precise amplitudes. The large discrepancy (a factor of 19) between the observed and predicted rates of radiative  $J/\psi$  decays makes a pure quarkonium radial excitation interpretation of  $\psi$  very unlikely.

It is an obvious question if a satisfactory solution can be found by mixing in a glueball state with the radial excitations, and identifying the predominantly  $1G$  state with the physical  $\psi$  as done above in the ground-state-only analysis. A reasonable fit to the  $\eta, \eta', \psi$  masses is given by diagonalising the full  $5 \times 5$  matrix of Table 11 with  $\beta = 153 \text{ MeV}/c^2$  (as in Table 5) and a somewhat larger value for  $M_G$  of  $1550 \text{ MeV}/c^2$ , all other parameters being the same as in the solution (43). The eigenvalues and eigenvectors are:

$$\begin{aligned} \eta_1(513) &= 0.728|\psi_1^{\text{NS}}\rangle + 0.07|\psi_2^{\text{NS}}\rangle - 0.647|\psi_1^{\text{S}}\rangle - 0.197|\psi_2^{\text{S}}\rangle - 0.086|G\rangle \\ \eta_1'(936) &= 0.612|\psi_1^{\text{NS}}\rangle - 0.268|\psi_2^{\text{NS}}\rangle + 0.695|\psi_1^{\text{S}}\rangle - 0.001|\psi_2^{\text{S}}\rangle - 0.265|G\rangle \\ \psi(1446) &= 0.108|\psi_1^{\text{NS}}\rangle - 0.681|\psi_2^{\text{NS}}\rangle - 0.088|\psi_1^{\text{S}}\rangle + 0.134|\psi_2^{\text{S}}\rangle + 0.706|G\rangle \\ \eta_2(1540) &= 0.007|\psi_1^{\text{NS}}\rangle + 0.230|\psi_2^{\text{NS}}\rangle + 0.238|\psi_1^{\text{S}}\rangle - 0.850|\psi_2^{\text{S}}\rangle + 0.41|G\rangle \\ \eta_2'(1958) &= 0.289|\psi_1^{\text{NS}}\rangle + 0.637|\psi_2^{\text{NS}}\rangle + 0.185|\psi_1^{\text{S}}\rangle + 0.470|\psi_2^{\text{S}}\rangle + 0.50|G\rangle \end{aligned} \quad (45)$$

The corresponding values of  $x_{\text{ef}}, y_{\text{ef}}$  for  $\eta_1, \eta_1'$  are shown in Table 12.

The general conclusion to be drawn from (43,45) and Table 12 is that predictions based on the non-strange or strange quarkonium content of the  $\eta$  and  $\eta'$  are little affected by radial mixing. This is illustrated in Table 13 where the predicted radiative width  $\Gamma_{\gamma\gamma}(\eta')$  given by the ground state only solution (Table 6), (43) and (45) are compared for the FC and IC models. For all three solutions the IC model is excluded by the experimental width.

In both of the solutions (43), (45) the  $\eta_2$  state has a relatively large production rate in radiative  $J/\psi$  decay. Solution (45) and (26) with  $\eta' \rightarrow \eta_2'$  gives:

$$\text{BR}(J/\psi \rightarrow \eta_2'(1958)\gamma) = 4.8 \times 10^{-3}$$

It is tempting to identify the  $\eta_2'$  with the spin-parity  $0^-$  enhancement in the  $1.5 - 1.9 \text{ GeV}/c^2$  mass region recently observed by the MARK III collaboration [76]. From the product branching ratio [76]:

$$\text{BR}(J/\psi \rightarrow x\gamma) \text{BR}(x \rightarrow \rho^0 \rho^0) = (7.7 \pm 3.0) \times 10^{-4}$$

(where  $x$  is the spin parity  $0^-$  projection of the  $\rho^0 \rho^0$  enhancement observed in the channel  $2\pi^+ 2\pi^-$ ) a lower limit for the branching ratio of an iso-spin zero state may be estimated:

$$\text{BR}(J/\psi \rightarrow x(1=0)\gamma) \geq (2.3 \pm 0.9) \times 10^{-3}$$

consistent with the prediction above for  $\eta_2'$ .

It should finally be pointed out that the solution (45) is in any case ruled out because it predicts, using (26) with  $\eta' \rightarrow \psi$  a value of

\*) Mixing with higher radial excitations may give an  $\eta_2'$  mass in better agreement with the observed enhancement than solution (45)

$\approx 10^{-6}$  for  $BR(J/\psi \rightarrow \eta(1446)\gamma)$ , a factor of  $2 \times 10^{-4}$  smaller than the experimental lower limit! As in (43) and for the same reason, the  $\eta_2$  state can also not be identified with the physical  $\eta$ .

The validity of the model can only be tested by making a much more detailed analysis than that presented here. A global fit varying  $\alpha$ ,  $\beta$ ,  $M_G$  taking into account higher radial excitations as well as finite width effects and relativistic corrections (which are expected to be more important for radial excitations than for the ground state) is needed. Such an investigation is beyond the scope of the present paper whose primary aim is to make a meaningful test of the quark charges.

The two essential conclusions of this brief study of effects of radially excited states are:

- i) A pure quarkonium radial excitation interpretation of the  $\eta(1450)$  is very unlikely.
- ii) Predictions sensitive to the quarkonium amplitudes in  $\eta(548)$ ,  $\eta'(958)$  are little effected by mixing with radial excitations.

A comparison of the present analysis with previous work on radial excitations in light mesons [72-74] will be given in Section 7 below.

## 6. TENSOR MESON ANALYSIS

### 6.1 Analysis Method

The relatively small mass splittings between the tensor mesons  $A_2$ ,  $f$ ,  $f'$ ,  $\theta$  and the consistent experimental values of  $\Gamma_{\gamma\gamma}(A_2, f, f')$ , which are summarised in Table 14, allow a more straightforward determination of the flavour mixing matrix than for the pseudoscalar mesons.

For the tensors the mass dependence of the wave function derivative at the origin can be safely neglected\*. The two measured ratios:

$$\Gamma_{\gamma\gamma}(f)/\Gamma_{\gamma\gamma}(A_2) = 3.4 \pm 0.5 \quad \Gamma_{\gamma\gamma}(f')/\Gamma_{\gamma\gamma}(A_2) = 0.13 \pm 0.06$$

$M_{\text{ns}} = M_{A_2}$ , and the masses of the  $f$ ,  $f'$ ,  $\theta$  states 1.270, 1.520, 1.720  $\text{GeV}/c^2$  [31,50] then completely determine the mass matrix (22) for a given quark charge assignment\*\*.

To test the quark charges the resulting flavour amplitudes are checked by phenomenological constraints obtained from:

- i) The experimental upper limit [14]:  
 $\Gamma_{\gamma\gamma}(\theta)BR(\theta \rightarrow K\bar{K}) \leq 0.3 \text{ keV} \quad (95\% \text{ C.L.})$

- ii) The ratio [31]:  
 $BR(J/\psi \rightarrow f'\gamma)/BR(J/\psi \rightarrow f\gamma) = 0.2 \pm 0.09$

- iii) The strong decay widths [31]

\* In fact  $SU(3)$  breaking in  $|\partial\psi/\partial r|_{r=0}$  is allowed for via (19b) but  $|\partial\psi_{\text{ns}}/\partial r|_{r=0}$  is taken to be the same for all states.

\*\* In practice a (zero constraint) fit was made to the two radiative width ratios by varying  $M_S$  and  $Z_T$  (as in the pseudoscalar case) to give  $\chi^2 = 0$ .

$$\begin{aligned}
\Gamma_{\pi\pi}(f) &= 149 \pm 17 \text{ MeV} \\
\Gamma_{KK}(f) &= 5.2 \pm 0.7 \text{ MeV} \\
\Gamma_{KK}(f') &= 59 \pm 10 \text{ MeV} \\
\Gamma_{\pi\pi}(f') &= 0.8 \pm 0.3 \text{ MeV}
\end{aligned}$$

The model for the strong decays is the same as that used to derive (27). For the FC model two additional phenomenological parameters are required, a reduced width  $\Gamma_0$  and an SU(3) breaking parameter  $\xi$  (see Fig. 7a). The model is further checked using the decays:

$$\begin{aligned}
K^{*0}(1420) &\rightarrow K\pi, K\eta, K^*(892)\pi, K\omega, K\rho \\
A_2(1310) &\rightarrow \pi\pi, KK
\end{aligned}$$

In this connection a solution of the problem of the 'anomalously large'  $f$  width, raised in [13] is proposed.

For the IC model a meaningful quark charge test must take into account the possibly dominant contribution from charged gluon annihilation to the  $2\gamma$  width\*. This is allowed for by a parameter  $\gamma$  defined so that (18) becomes:

$$\Gamma_{\gamma\gamma}(f) = \frac{1152\pi^2}{5} \sum_{i=1}^8 Q_i^2 \left[ \dots \right] + \frac{\sqrt{3}}{2} \gamma \sum_{i=1}^8 Q_i^2 \left| \frac{\partial \psi}{\partial r} \right|_{r=0} \quad (46)$$

Here  $Q_{g_i}^2$  is the gluon charged squared (4 of the 8 gluons in IC models have charge  $\pm e$ ). Since in the IC model large gluonium amplitudes are found in the  $f, \theta$  for some  $\gamma$  values a further parameter  $r$  defined as:

$$r \equiv \frac{\langle \pi^+ \pi^- | T | G \rangle}{\langle \pi^+ \pi^- | T | ns \rangle} = \frac{\langle K^+ K^- | T | G \rangle}{\langle K^+ K^- | T | ns \rangle} \quad (47)$$

\*) Recall that  $g^+ g^-$  annihilation is allowed in S-wave for  $J^P = 2^+$ , whereas  $q\bar{q}$  annihilation must be at least P-wave, implying that  $\psi(0)$  vanishes in this case.

is required to describe the strong decays in (iii) above. Eqn. (47) assumes SU(3) invariance. Consistent with this  $\xi$  is also set equal to unity for the IC model analysis. Including SU(3) breaking ( $\approx 20\%$  correction) is not expected to change the overall conclusion of the IC analysis presented below.

The procedure to test the IC model is then as follows:

- The mass matrix and hence the flavour wave functions are determined as described above for a given value of  $\gamma$ .
- The experimental widths  $\Gamma_{\pi\pi}(f), \Gamma_{\pi\pi}(f')$  are used in (49) below to determine the parameters  $\Gamma_0, r$ .
- The predicted values of  $\Gamma_{KK}(f), \Gamma_{KK}(f')$  (using (49)) and  $\Gamma_{\gamma\gamma}(\theta)BR(\theta \rightarrow KK)$  (using (46,51)) are compared with the experimental measurements in (iii, i) above.
- $\gamma$  is varied through an arbitrary range  $\geq 0$  so as to fit (if possible) the 3 experimental widths in (c).

## 6.2 Results for Fractional Quark Charges

The flavour wave functions of the  $f, f', \theta$  determined as described above are presented in the first 3 rows of Table 15. It can be seen that  $f, f'$  are predicted to be almost ideally mixed states:

$$\begin{aligned}
|f\rangle &= |ns\rangle = \frac{1}{\sqrt{2}} (|u\bar{u}\rangle + |d\bar{d}\rangle) \\
|f'\rangle &= -|s\rangle = -|s\bar{s}\rangle
\end{aligned}$$

The  $\theta$  is essentially decoupled from quarkonium. Although this may be consistent with  $\theta$  being an almost pure glueball, no constraints on the branching ratios can be obtained by considering interference between the gluonium and quarkonium components of  $\theta$  as in [10]. Another consequence of the weak mixing is that if the  $\theta$  is mainly glueball the 'bare'  $2^+$  glueball mass must be very close to the physical  $\theta$  mass.

The mixing parameters are small:



$$\alpha = -23 \text{ MeV}/c^2 \quad \beta = 5 \text{ MeV}/c^2$$

while the SU(3) breaking parameter  $Z_T$  is found to be 0.34, considerably smaller than the QCD prediction of 0.53 in Table 3. As the mixing amplitudes are so small the solution is, however, relatively insensitive to the value of  $Z_T$ .

$M_S$  is found to be  $1.525 \text{ GeV}/c^2$  in good agreement with the expectation:

$$M_S = 2 M_{K^{*-}} - M_{A_2} = 1.540 \text{ GeV}/c^2$$

of naive quark counting. This is consistent with SU(3) breaking in the tensor mesons being dominated by the non-strange strange quark mass difference, leading to the observed ideal mixing.

Also shown in Table 15 are the solutions obtained when corrections are applied for:

i) SU(2) breaking corrections [82]

or

ii) relativistic corrections [7].

In i), following [82] the  $|ns\rangle$  component of the  $f$ , and the isospin one  $A_2$  wave function are replaced by:

$$\begin{aligned} |ns'\rangle &= \frac{1}{\sqrt{2}} (1.05|u\bar{u}\rangle + 0.95|d\bar{d}\rangle) \\ |A_2'\rangle &= \frac{1}{\sqrt{2}} (0.95|u\bar{u}\rangle - 1.05|d\bar{d}\rangle) \end{aligned} \quad (48)$$

For ii) relativistic correction factors of 0.24 were applied to (18) for the  $f$ ,  $A_2$  and 0.36 for  $f'$  [7]. Neither SU(2) breaking, nor relativistic corrections change the almost pure ideal mixing pattern for  $f$ ,  $f'$  with weak quarkonium admixtures in the  $\Theta$ .

The relations used to describe the strong decays  $T \rightarrow PP$  are [10,13]:

$$\Gamma_{\pi\pi}(f) = \Gamma_0 (x_f + rz_f) \quad (49a)$$

$$\Gamma_{KK}(f) = \frac{\Gamma_0}{3} \frac{K}{K'} (\xi x_f + \sqrt{2} y_f + 2rz_f) \quad (49b)$$

$$\Gamma_{\pi\pi}(f') = \Gamma_0 \frac{\pi}{K'} (x_{f'} + rz_{f'}) \quad (49c)$$

$$\Gamma_{KK}(f') = \frac{\Gamma_0}{3} \frac{K}{K'} (\xi x_{f'} + \sqrt{2} y_{f'} + 2 rz_{f'}) \quad (49d)$$

where  $r$  is defined in (47) and  $\xi$  in Fig. 7a. The  $K$  factors are  $\sim p_{cm}^5$  and account for phase space and a D-wave angular momentum barrier. Eqns (49) are, except for the inclusion of the SU(3) breaking parameter  $\xi$ , identical to those used in [10].

For the FC model  $z_{f,f'}$  are negligibly small so that (49) are independent of  $r$  in this case. Using the solution in the first three rows of Table 14 a satisfactory fit ( $\chi^2 = 3.8, 2 \text{ D.O.F.}$ ) is obtained to the widths in (49) with:

$$\Gamma_0 = 146 \pm 6 \text{ MeV} \quad \xi = 0.89 \pm 0.06$$

The fitted and experimental values are compared in Table 16. This solution also predicts (from (26) with the replacements  $\eta' \rightarrow f', \eta \rightarrow f'$ ):

$$\frac{\text{BR}(J/\psi \rightarrow f'\gamma)}{\text{BR}(J/\psi \rightarrow f\gamma)} = 0.15$$

in good agreement with the experimental value (ii) in Section 6.1).

The measured width  $\Gamma_{KK}(f')$  in Table 16 is derived from the experimental full width  $67 \pm 10 \text{ MeV}$ \* corrected for the measured  $\Gamma_{\pi\pi}(f')$  and for  $\Gamma_{\pi\pi}(f')$  which is estimated using the relation analogous to (49):

\* This value is consistent with the 1980, 1984 particle data group values. In [31] a significantly larger value of 75 MeV was given.

$$\Gamma_{\eta\eta}(f') = \frac{\Gamma_0^{K'}}{12} \frac{K'}{K_\pi} (x_{f'} + \sqrt{2} \xi y_i) \quad (50)$$

In (50) the  $\eta$  wave function is approximated by:

$$|\eta\rangle = \frac{1}{\sqrt{2}} (|ns\rangle - |s\rangle)$$

which is close to the fit solution in Table 6.  $\Gamma_{\eta\eta}(f')$  is estimated to be 7 MeV, corresponding to a 10 % branching ratio of  $f'$  into  $\eta\eta$ .

Also shown in Table 16 are experimental and predicted decay widths of several other processes of the type  $T \rightarrow PP$  and  $T \rightarrow PV$  calculated using formulae similar to (49,50). For the  $T \rightarrow PV$  decays the  $A_{2 \rightarrow \pi\pi}$  decay is used as input and a D-wave barrier-phase space factor  $\approx p_{CM}^5$  is included. Of the eight predictions, six are in reasonable agreement with experiment, and one,  $\Gamma_{\eta\eta}(f')$  is as yet untested. The predicted value of  $K^{*0} \rightarrow K\pi$ , however, lies a factor of 1.6 above the experimental measurement, well outside the range of errors.

Rosner in [13] used a similar model to predict  $\Gamma_{\pi\pi}(f)$  using  $\Gamma_{K\pi}(K^{*0})$  as input, and concluded that the former is anomalously large. In [13] this was explained by the hypothesis of a glueball component of the  $f$  interfering constructively with the quarkonium component in the  $\pi\pi$  decay mode. The  $K^{*0} \rightarrow K\pi$  decay differs, however, from  $f \rightarrow \pi\pi$  in that a number of different final states with the same flavour content as  $K\pi$  is quite large. In fact the channels  $K^*\pi$ ,  $K^*\pi\pi$ , and  $K\rho$  all have appreciable branching ratios. In contrast, in the  $f$  decay, the only competing channel is  $4\pi$  which is strongly suppressed by phase space factors. The low observed rate for  $K^{*0} \rightarrow K\pi$  may then be a consequence of unitarisation corrections (final state scattering effects) among the channels  $K\pi$ ,  $K^*\pi$ ,  $K^*\pi\pi$ ,  $K\rho$ ; the  $K\pi$  channel being preferentially absorbed into the other channels. It is interesting to note that the sum of all the predictions for the various decay channels of  $K^{*0}$  in Table 16 is 106 MeV in excellent agreement with the measured total width of  $100 \pm 10$  MeV [31].

In conclusion the flavour amplitudes found from the measured  $2\gamma$  widths of  $f$ ,  $f'$ ,  $A_2$  and (18) give, in the FC model, a good description of

both the strong  $f$ ,  $f'$  decays and the ratio of the radiative decays of  $J/\psi$  into  $f'$  and  $f$ . As the  $\theta$  is effectively decoupled from the ground state quarkonium sector a pure glueball interpretation is possible. It could also, however, be a radially excited quarkonium state that does not mix with the ground state, or some other weakly mixed exotic state such as  $q^2 \bar{q}^2$  [84]. Hyperfine mixing with radial excitations should be strongly suppressed because of the vanishing of the wave function at the origin in the tensor states. The ideal mixing found in the ground state also indicates that gluonium annihilation mixing should also be weak for radial excitations.

Finally it may be remarked that the weak gluonium amplitude found here in the  $f$  is inconsistent with the solution proposed in [85] to explain the 'anomalous' decay angular distribution of the  $f$  produced in radiative  $J/\psi$  decays [86].

### 6.3 Results for Integral Quark Charges

The gluonium amplitudes,  $z$ , found for the  $f$ ,  $f'$  and  $\theta$ , from the measured ratios  $\Gamma_{\gamma\gamma}(f)/\Gamma_{\gamma\gamma}(A_2)$ ,  $\Gamma_{\gamma\gamma}(f')/\Gamma_{\gamma\gamma}(A_2)$  are shown as a function of the parameter  $\gamma$  of (46) in Fig. 9. Small values of  $\gamma$  give large gluonium amplitudes in the  $f$ ,  $f'$ . For large  $\gamma \gtrsim 10$  the  $\theta$  approaches a pure glueball state.  $\Gamma_{\gamma\gamma}(\theta)$  given by (46) taking as input the measured value of  $\Gamma_{\gamma\gamma}(f)$  is shown as a function of  $\gamma$  in Fig. 10.

To compare with the experimental upper limit on  $\Gamma_{\gamma\gamma}(\theta)BR(\theta \rightarrow KK)$  [14], the partial width for  $\theta \rightarrow KK$  is found using

$$\Gamma_{KK}(\theta) = \frac{\Gamma_0}{3} \frac{K}{K_\pi} (x_\theta + \sqrt{2} y_\theta + 2 rz_\theta) \quad (51)$$

with  $\Gamma_0$ ,  $r$  determined from the experimental widths  $\Gamma_{\pi\pi}(f)$ ,  $\Gamma_{\pi\pi}(f')$ , and (49a,c) with  $\xi = 1$ . The dependence of  $\Gamma_{\gamma\gamma}(\theta)BR(\theta \rightarrow KK)$  on  $\gamma$  is given in Fig. 11. The 95 % C.L. upper limit of 0.3 keV [14] gives a similar limit on  $\gamma$  of 0.5.

The corresponding predicted values for  $\Gamma_{KK}(f)$ ,  $\Gamma_{KK}(f')$  as a function of  $\gamma$  found using (49b,d) are compared with experiment in Fig. 12a,b. The prediction for  $\Gamma(f \rightarrow KK)$  lies within 2 $\sigma$  of experiment only for  $\gamma > 5$ . This would give  $\Gamma_{\gamma\gamma}(\theta)BR(\theta \rightarrow K\bar{K}) > 2$  keV in contradiction with [14].

The IC model is, therefore excluded by the experimental values of  $\Gamma_{\gamma\gamma}(\theta)BR(\theta \rightarrow K\bar{K})$ ,  $\Gamma_{KK}(f,f')$  for all values of  $\gamma$ .

## 7. DISCUSSION

As the analysis of  $2\gamma$  radiative widths presented here uses the non-relativistic quarkonium annihilation formulae (17,18) it is important to examine the validity of such a description for light meson systems.

Eqn (17) assumes a factorisation between a short distance annihilation process and a flux factor, proportional to  $|\psi(0)|^2$ , giving the probability that the quark anti-quark pair find themselves at small mutual separation. This will be a good approximation if the typical range of the annihilation process  $\Delta$  is very much smaller than  $r$ , the mean radius of the  $q\bar{q}$  system. A parameter of merit for the applicability of (17) is, therefore,  $\Delta/r$ , which should be small for the quarkonium description to be valid. The parameter  $\Delta^2$  is of the order of the inverse of the quark propagator:

$$m_q^2 + M^2/4$$

and so can be estimated from the mass of the state and the appropriate constituent quark mass. For harmonic oscillator wave functions the mean radius of the  $q\bar{q}$  system is:

$$\bar{r} = (2/\pi) \psi(0)^{-2/3} \quad (52)$$

Values of  $\Delta/r$  for the  $2\gamma$  decays of singlet positronium,  $\eta_b$ ,  $\eta_c$ ,  $\eta'$ ,  $\eta$  and  $\pi^0$  are presented in Table 17. For positronium, the Bohr radius is taken for  $\bar{r}$ .  $\psi(0)$  for  $\eta_b$ ,  $\eta_c$  is estimated from the leptonic widths of  $\mathcal{N}, \mathcal{J}/\psi$  using (10a), but including the first order QCD correction as in (31). For  $\eta$ ,  $\eta'$   $\psi(0)$  is given by (29-31), while for the  $\pi^0$  the value derived from the experimental pion charge radius [39,87] is taken:

$$\psi(0)^{2/3} = \left[ \frac{1}{2} \left( \frac{3}{2\pi} \right)^{1/2} \frac{1}{\langle r^2 \rangle^{1/2}} \right] = 104 \text{ MeV} \quad (53)$$

To calculate  $\Delta$ , masses of 1.85, 5.0 GeV/ $c^2$  are taken for  $c$ ,  $b$  quarks.

It can be seen from Table 17 that the difference in  $\Delta/r$  between heavy and light quark systems is not large. There is a factor  $\approx 2$  between  $c\bar{c}$  and the light quark states which have similar values  $\approx 0.45$ . The difference between even  $b\bar{b}$  and positronium is, however, much larger, a factor  $\approx 100$ . As the ground state S-wave function peaks at the origin, large values of  $\Delta/r$  should reduce the flux factor and hence the radiative width. However, the  $\eta, \eta'$  have similar values of  $\Delta/r$ , so this suppression factor should largely cancel in the ratio of  $\Gamma_{\gamma\gamma}(\eta')$  to  $\Gamma_{\gamma\gamma}(\eta)$  which is used to estimate the exponent  $n$  in (29).

The work presented here differs from more general analyses, previously published (for example [12,35,36]) which aimed to fit the entire mass spectrum of light meson states, in that experimental constraints are more rigorously applied to specific states ( $\eta, \eta'$  and  $f, f'$ ), and that the number of adjustable parameters is kept to the absolute minimum. In [12] 45 different state masses were fitted, but 11 adjustable parameters are used to describe only the potential. In the present analysis, taking the quark masses as fixed by baryon magnetic moments [40], for the pseudo-scalars, 13 experimental quantities (3 masses, 5 ratios of  $1\gamma$  widths, 2 ratios of strong interaction processes and 3  $2\gamma$  decay widths) are described by 5 parameters:  $\alpha, \beta, Z_p, M_{ns}, n$ . Since, however,  $M_{ns}$  can be independently estimated (Section 5.7 above) and the SU(3) breaking parameter agrees well with the perturbative QCD estimate (23a), the only really 'free' parameters are  $\alpha, \beta, n$ .

For the tensors 14 experimental quantities (3 masses, two ratios of  $2\gamma$  radiative widths, 1 ratio of  $1\gamma$  widths and 8 strong decay widths) are described by 6 parameters  $\alpha, \beta, Z_p, M_{ns}, \Gamma_0, \xi$ . Experiment is, in fact, equally well described by the pure quarkonium solution with  $\alpha = \beta = \beta Z_T = 0$ , in which case there is only one adjustable parameter  $\Gamma_0$ , since  $M_{ns}$  agrees well with the quark counting estimate and, as will now be shown  $\xi$  can also be estimated from a simple perturbative QCD argument.

If the duality diagrams in Fig. 7a are replaced by the lowest order QCD diagrams the 'sea' quark pair will result in each case from a single gluon coupling. This implies:

$$\xi = \left| \frac{\alpha_S(m_S)}{\alpha_S(m_{ns})} \right|^{1/2} \quad (54)$$

which gives  $\xi = 0.86$  for  $\Lambda = 90 \text{ MeV}/c^2$ , in good agreement with the fitted value of  $0.89 \pm 0.06$ .

It is the inclusion of large SU(3) breaking corrections that distinguishes the present work from previous studies of quarkonium gluonium mixing [8,9,10,13]. Stanley and Robson [12] have already realised that such corrections are the key to solving the  $\eta, \eta'$  mixing problem using a linear mass matrix. They did not, however, allow in their analysis the possibility of explicit gluonium admixtures and neglected QCD radiative corrections. A very rapid dependence of the mixing matrix for the isospin zero pseudoscalar mesons [40] on the mass of the state is not supported by the present analysis. In fact a solution almost identical to that in Table 6 is given by replacing the factors depending on  $M_p$  in (23a) by unity. The SU(3) breaking parameter  $Z_p$  must, however, be significantly less than unity.

The good agreement found between the fitted values of  $Z_p, \xi$  and the naive perturbative QCD predictions may seem, at first sight, fortuitous as conventional wisdom would say that such perturbative calculations, which may be of only doubtful validity for the charmonium and bottomium systems, are completely inapplicable to light quark systems. As previously pointed out by Paschalis and Gounaris [39], however, the important parameter is the ratio of  $\Lambda$  to the lightest constituent quark mass  $m_{ns}$ . As quarks always appear 'dressed' in hadrons it is clearly this mass, and not the current mass of the QCD Lagrangian which is appropriate here. If  $\Lambda$  is indeed as low as  $90 \text{ MeV}$  as indicated by QCD analyses of the  $c\bar{c}$  and  $b\bar{b}$  systems [42],  $\alpha_S(m_{ns})$  is still a 'small' number and perturbative calculations may still be expected to have an approximate validity, even for light quark systems. It will now be shown, from general arguments that  $Z_p$  is a privileged parameter in this respect, in that it is expected to be particularly insensitive to higher order QCD corrections, even though  $\alpha_S(m_{ns}) \approx 0.4$ .

To second order in QCD  $Z_p$  is given by:

$$Z_p = \frac{\alpha_s(m_s)}{\alpha_s(m_{ns})} \frac{[1 + C(m_{ns}, m_s, M) \alpha_s(m_s) \alpha_s(m_{ns})] \left[ \frac{m_s}{m_{ns}} \right]^{3/4}}{[1 + C(m_{ns}, m_s, M) \alpha_s(m_s)^2] \left[ \frac{m_s}{m_{ns}} \right]} \quad (55)$$

The second order QCD correction corresponds to four gluon exchange, and the function C depends on the relative strength of the two gluon and four gluon amplitudes. The mathematical form of (55) implies that the second order QCD correction to  $Z_p$  is small even though  $\alpha_s(m_s)$ ,  $\alpha_s(m_{ns})$  may be quite large. With  $\alpha_s(m_{ns}) = 0.43$ ,  $\alpha_s(m_s) = 0.31$  and  $C = \text{const} = 1$  the second order correction is only 4 %. Even in the pathological case when  $C \rightarrow \infty$  the second order correction is only 26 %. A similar argument can be given for the insensitivity of  $\xi$  to higher order corrections.

If the comparison between the fitted values of  $Z_p$  and  $\xi$  and the QCD predictions is taken seriously the scale parameter  $\Lambda$  can be estimated. The fitted value of  $Z_p$  compared to (23a) gives:

$$\begin{aligned} \Lambda &= 135 \pm 7 \text{ MeV}/c \\ \Lambda &\leq 148 \text{ MeV}/c \quad 95 \% \text{ C.L.} \end{aligned}$$

whereas  $\xi = 0.89 \pm 0.06$  and (54) gives

$$\begin{aligned} \Lambda &= 70^{+45}_{-60} \text{ MeV}/c \\ \Lambda &\leq 150 \text{ MeV}/c^2 \quad 95 \% \text{ C.L.} \end{aligned}$$

In view of the dependence of the propagator and wave function factors in (23a) on the constituent quark masses, the quoted errors and upper limits, derived only from the statistical errors on the fitted quantities should be treated with caution. However:

$$\Lambda = 100 \pm 50 \text{ MeV}/c$$

would seem to be a reasonable estimate from the internal consistency of the two estimations with:

$$\Lambda \leq 200 \text{ MeV}/c$$

as a conservative upper limit. Both the value and the error on these estimates of the scale parameter of QCD compare quite favourably with other estimates from gluon production in  $e^+e^-$  annihilation, structure functions and heavy quarkonia [42].

The parameter with the least clear physical interpretation in the pseudoscalar meson analysis is the exponent n describing, in a static non-relativistic model the mass dependence of  $|\psi(0)|^2$ . Interpreting the mass of the state as proportional to a reduced mass  $\mu$  (not evidently a valid procedure in states where binding energies are so large), then  $n = 2.6 \pm 0.3$  is close to the  $\mu^3$  scaling law of a Coulomb potential [44]. On the other hand  $c\bar{c}$ ,  $b\bar{b}$  quarkonia [75] as well as the masses of the isospin one states  $\pi$ ,  $\pi'$ ,  $\rho$ ,  $\rho'$  (Table 10) favour a near logarithmic potential giving a  $\mu^{3/2}$  law for  $|\psi(0)|^2$ . A steeper mass dependence than this corresponding to a singular potential (see Table 10) would contradict QCD expectations as such potentials are expected to become dominant at short distances, for quarkonia heavier than  $b\bar{b}$ , certainly not for light quarks.

The mass dependence described by the exponent n should then rather be interpreted as that of the relativistic correction to  $|\psi(0)|^2$ . Formulae relating the non-relativistic wave function at the origin  $\psi^{NR}(0)$  to the fully relativistic Bethe Salpeter wave function  $\psi^{BS}(0)$  have recently been obtained by Durand and Durand [88]. For S-wave  $q\bar{q}$  states of mass  $M \leq 2 m_q$  it is conjectured that:

$$\left| \frac{\psi^{BS}(0)}{\psi^{NR}(0)} \right|^2 = \frac{M^2}{4m_q^2} \left| \frac{\psi^{NR}(0)}{\psi(0)} \right|^2 \quad (56)$$

If the  $\psi^{NR}(0)$  is estimated from the pion charge radius using (53) (which is based on a static derivation of  $\langle r^2 \rangle^{1/2}$ , using harmonic oscillator wave functions [39]) then, on replacing the non-relativistic wave function in (32) by the Bethe Salpeter wave function from (56),  $\Gamma_{\gamma\gamma}(\pi^0) = 4.0, 7.2 \text{ eV}$  for  $m_{\eta_s} = 336, 300 \text{ MeV}/c^2$  which may be compared\* with the

\* Note that (32,56) give a dependence of  $\Gamma_{\gamma\gamma}(\pi^0)$  on the constituent quark mass (which is known to a precision of only  $\approx 10$ -20 %) of  $(m_{ns})^{-6}$ !

experimental value of  $7.85 \pm 0.55$  eV [31]. In addition the value of  $n$  of  $2.6 \pm 0.3$  given by (17,29) and the experimental ratio  $\Gamma_{\gamma\gamma}(\eta')/\Gamma_{\gamma\gamma}(\eta)$  (indicating that  $\psi_{n1}^{NR}(0) \approx \psi_{n0}^{NR}(0)$ ) is consistent with (56) and supports the interpretation of the strong dependence of the radiative widths of light mesons on the mass of the state, (used as an ansatz in previous purely phenomenological analyses [37,38,62]), as being due to relativistic corrections. It is clearly of interest to have a proof of (56). A similar relation for  $M \geq 2 m_q$  is proved in [88].

In the quark charge test  $n$  is only needed to estimate the small change in  $|\psi(0)|^2$  in passing from the  $\omega$  to the  $\eta'$  mass. In this case the discrimination between the FC and IC models is very insensitive to the value of  $n$ . If this correction to  $|\psi(0)|^2$  is neglected  $\Gamma_{\gamma\gamma}(\eta')$  is found to be 3.3, 14.3 keV for the FC, IC models, respectively, still strongly favouring the FC model.

There are several differences between the analysis of radial mixing presented in Section 5.7 above and the work of Frank and O'Donnell [72-74]. Specifically, in [72-74]:

- i) SU(3) breaking is neglected.
  - ii) Annihilation mixing via the operator  $Q_G$  of different radial excitation states is neglected.
  - iii) The choice of a harmonic oscillator potential gives a wave function at the origin that increases with principal quantum number,  $|\psi_{n+1}(0)| > |\psi_n(0)|$  thus favouring stronger mixing of higher radial excitations.
  - iv) In [74] the decays  $J/\psi \rightarrow P\gamma$  are assumed to be mediated only by the gluonium component of the pseudoscalar meson wave function.
- Concerning ii), explicit evaluation of the mixing matrix (Table 11) shows that in the present analysis the neglected mixing amplitudes are large. In particular the important cancellation between the contributions of  $Q_{HF}$  and  $Q_G$  is not accounted for in [72-74].

The choice of a harmonic oscillator potential iii) gives a poor fit to the  $\pi - \pi'$ ,  $\rho - \rho'$  mass differences. In [73] the predicted values of  $m_{\pi'}$ ,  $m_{\rho'}$  lie, respectively 2, 3 standard deviations below the experimental values [31].

As for (iv) the work presented here indicates, on the contrary, that radiative  $J/\psi$  decays into  $\eta$ ,  $\eta'$  are dominated rather by the quarkonium component of the wave function.

For the tensor mesons the results of the present analysis may be compared to those of Rosner and Tuan [10]. With fractional quark charges a good description is here obtained of the  $2\gamma$  decay widths of  $f$ ,  $f'$ ,  $A_2$  and of the strong decay widths for  $f$ ,  $f' \rightarrow \pi\pi$ ,  $K\bar{K}$  which were originally proposed in [10] to constrain possible solutions. The main difference from [10] is that  $\theta$  is here found to be almost completely decoupled from the quarkonium sector, so that no light is shed by the solution on the strong decays of the  $\theta$ . The question of the nature of the  $\theta$ : glueball, radial excitation, 4 quark state, ... is left open.

The IC model (always in the limit  $m_g^2 \gg \langle q^2 \rangle$ ) is excluded by the tensor meson analysis as no solution can be found which is consistent with the  $f$ ,  $f'$ ,  $A_2$   $2\gamma$  widths,  $f$ ,  $f' \rightarrow \pi\pi$ ,  $K\bar{K}$  and the experimental upper limit on  $\Gamma_{\gamma\gamma}(\theta)BR(\theta \rightarrow K\bar{K})$ .

In summary the results presented in Sections 5.5, 6.2, 6.3 strongly favour the FC model, always with the caveat that the effective gluon mass is not  $\lesssim 1$  MeV/c<sup>2</sup>. In conclusion, brief mention is made of other recent experiments or analyses relevant to the discrimination between gauge IC and FC quark models.

In [34] I suggested the use of a sum rule due to Worden [89] in a resonance saturation approximation to determine  $\Sigma Q_q^4$  and hence test the quark charges. In [34] it is wrongly stated that the recent measurements of  $2\gamma$  widths when used in the sum rule favour the IC model. After correcting a sign error in the contribution from the charged pion Born term and adding, for the IC case, the contribution from the charged gluon box diagram, it is found that the sum rule is equally valid in the FC and IC models and so does not discriminate between them.

Jayaraman and Rindani [94] have recently calculated the cross section for the semi-inclusive process

$$pp \rightarrow \gamma\gamma X$$

where both photons are produced at large momentum transfer. The subprocesses contributing are:

$$q\bar{q} \rightarrow \gamma\gamma, \quad g^+g^- \rightarrow \gamma\gamma$$

(the second for the IC model only). The single experimental measurement of the process from the ISR at CERN [95] is found to agree well with the FC model prediction. In the IC model, however, a very large contribution from charged gluon annihilation is found which, depending on the detailed parameterisation of the gluon structure functions, predicts a cross section which is a factor of 30 to 50 greater than the experimental measurement.

The overall conclusion from the analysis of these two experiments using real photons, and of this paper is the same: quarks have fractional charges, even when they couple to pairs of massless photons.

#### Acknowledgements

I should like to specially thank J.M. Levy for many fruitful and informative discussions about many aspects of the work presented here. I thank also to S. Rindani for several clarifying remarks on the gauge integer charge quark models. Critical remarks by S.J. Brodsky and P. Zerwas on the non relativistic quark model, and by F. Gutbrod on the linear mass mixing problem have helped to improve my understanding in these areas. A discussion with G. Mennessier on the strong decays of the tensor mesons is also gratefully acknowledged. Finally I should like to thank D. Olivier for a careful reading of the manuscript and for informing me of recent work on relativistic corrections in the decays of quarkonia.

A number of studies have been made [24-26,90] of high  $P_T$  jet production in singly tagged  $\gamma\gamma$  collisions in the context of the gauge IC models. The most recent of these [26] concluded that the  $q^2$  dependence of recent PLUTO data is consistent with the IC model provided that  $m_g$  lies in the interval 150 to 350 MeV/c<sup>2</sup>. This is in contradiction with the result of the present study using  $\Gamma_{\gamma\gamma}(n')$  (Fig. 8). The difficulty of this type of analysis (as clearly pointed out in [26]) is to extract the contribution of the  $\gamma\gamma \rightarrow q\bar{q}, \gamma\gamma \rightarrow g^+g^-$  terms, which alone are sensitive to the quark charges, from higher order QCD processes [91], higher twist processes [92] or simply the tail of the diffractive distribution. At the time of writing no detailed comparison of experimental data with these conventional sources of high  $P_T$  events, over and above the Born term  $\gamma\gamma \rightarrow q\bar{q}$  has been made. It is perhaps more prudent to await the results of such an analysis before interpreting an experimental excess in terms of the IC model.

The main limitation of the present analysis (and also of [24-26,90]) is due to the virtuality of the photons when  $2\gamma$  collisions are investigated at  $e^+e^-$  colliders. Definite exclusion of gauge IC models (not as done here, the establishment of a stringent upper limit on  $m_g$ ) requires a process involving two real photons, so that the 'propagator suppression' factor of (1) is absent.

A recent CERN experiment [93] has studied the inclusive process:

$$\gamma Li^6 \rightarrow \gamma X$$

where the final state photon is produced at large momentum transfer ( $> 2$  GeV/c). The aim was to isolate the parton level subprocess:

$$\gamma q \rightarrow \gamma q$$

whose amplitude contains the coupling to a quark of two real photons and so is proportional to  $Q_q^2$  as given by (5). The results of this experiment are consistent with the FC model, after allowing for higher order QCD corrections, thus strongly disfavours the IC model.

TABLE 1  
Values of  $q_i^2$ 

Flavour	FC	IC*
u, c, ...	$\frac{4}{3}$	2
d, s, b, ...	$\frac{1}{3}$	1

\*)  $q_1^2, q_2^2 \ll m_g^2$  assumed in (5)

TABLE 2  
Values of  $S_j$  (see Eqns (12,13))
$$S_j = \sum_{\alpha} \sum_i A_{\alpha i}^j Q_{\alpha i}^2$$

FC	IC*
$\frac{1}{\sqrt{2}}$	$\frac{1}{\sqrt{2}}$
$\frac{1}{\sqrt{6}}$	$\frac{1}{\sqrt{6}}$
$\frac{2}{\sqrt{3}}$	$\frac{4}{\sqrt{3}}$

\*)  $q_1^2, q_2^2 \ll m_g^2$  assumed in (5)

TABLE 3  
Lowest Order Factorised QCD Predictions  
for SU(3) breaking parameters

State	$Z(M_j)$
$\eta$	0.57
$\eta'$	0.73
$\tau$	0.86
f	0.79
f'	0.77
$\theta$	0.73

$Z_p = 1.04$   
 $Z_T = 0.53$

TABLE 4  
Results of the Global Fit to the  $\eta, \eta', \tau$  Mass Matrix  
I. Physical Constraints

Physical Constraint	Experimental Value	Fit Value
$\frac{\Gamma(\rho \rightarrow \pi\pi)}{\Gamma(\omega \rightarrow \pi\pi)}$	$ x_{\eta} ^a = 0.73 \pm 0.10$	$0.67 \pm 0.03$
$\frac{\Gamma(\eta' \rightarrow \rho\gamma)}{\Gamma(\omega \rightarrow \pi\pi)}$	$ x_{\eta'} ^a = 0.63 \pm 0.12$	$0.50 \pm 0.04$
$\frac{\Gamma(\phi \rightarrow \pi\gamma)}{\Gamma(\omega \rightarrow \pi\pi)}$	$ y_{\eta} ^a = 0.74 \pm 0.06$	$0.73 \pm 0.03$
$\frac{\Gamma(A_2 \rightarrow \eta\pi, b)}{\Gamma(A_2 \rightarrow KK)}$	$3.0 \pm 0.4$	$3.2 \pm 0.3$
$\frac{\Gamma(\psi \rightarrow \eta'\gamma, b)}{\Gamma(\psi \rightarrow \pi\pi)}$	$4.2 \pm 0.7$	$4.2 \pm 0.7$

a) Values from Ref. [9]

b) Values from Ref. [31]

TABLE 5  
Results of the Global Fit to the  $\eta, \eta', \tau$  Mixing Matrix  
II. Mixing Matrix Parameters

	$M_{\eta\eta}$	$M_S$	$M_G$	$\alpha$	$\beta$	$Z_p$
	0.135	$0.67 \pm 0.01$	$1.22 \pm 0.05$	$0.360 \pm 0.018$	$0.1527^{+0.0004}_{-0.005}$	$0.89 \pm 0.03$
	GeV/c <sup>2</sup> (Input)	GeV/c <sup>2</sup>	GeV/c <sup>2</sup>	GeV/c <sup>2</sup>	GeV/c <sup>2</sup>	

All errors are purely statistical, quoted for  $\chi^2 = \chi_{\min}^2 + 1$



TABLE 8 Predictions for the Two Photon Radiative Widths of the  $\pi^0$ ,  $\eta'$  and  $\iota(1450)$

	FC	IC	FC	FC	FC	FC	Experiment
			$\Gamma_{\gamma\gamma}(\eta)$ from Ref. [74]	$\Gamma_{\gamma\gamma}(\eta)$ from Ref. [73]	no QCD correction	pure quarkonium in $\eta, \eta'$	
$\Gamma_{\gamma\gamma}(\pi^0)$ (eV)	4.4 $^{+3.6}_{-1.8}$	.71 $^{+65}_{-29}$	0.76 $^{+0.57}_{-0.29}$	28 $^{+39}_{-14}$	2.9 $^{+2.0}_{-1.2}$	9.0 $^{+5.0}_{-4.0}$	7.85 $\pm 0.55$
	6.8 $^{+5.6}_{-2.8}$ <sup>a)</sup>				4.5 $^{+3.1}_{-1.9}$ <sup>a)</sup>		
$\Gamma_{\gamma\gamma}(\eta')$ (keV)	5.5 $\pm 1.1$	17.6 $\pm 3.6$	6.7 $\pm 1.1$	4.4 $\pm 0.9$	5.9 $\pm 1.2$	8.5 $\pm 1.7$	4.5 $\pm 0.4$
$\Gamma_{\gamma\gamma}(\iota)$ (keV)	10 $\pm 3$	3.7 $\pm 1.1$	19 $\pm 5$	5.2 $\pm 1.6$	10 $\pm 3$	-	$\leq 17$ <sup>b)</sup>

a)  $m_{ns} = 300 \text{ MeV}/c^2$       b)  $BR(\iota \rightarrow K\bar{K}\eta) = 0.42$

62.

TABLE 6 Results of the Global Fit to the  $\eta, \eta', \iota$  Mixing Matrix  
III. Flavour Amplitudes

	x	y	z
$\eta$	0.67 $\pm 0.03$	-0.73 $\pm 0.03$	-0.135 $\pm 0.008$
$\eta'$	0.50 $\pm 0.04$	0.61 $\pm 0.05$	-0.62 $\pm 0.08$
$\iota$	0.53 $\pm 0.05$	0.45 $\pm 0.06$	0.72 $\pm 0.07$

Errors are purely statistical, quoted for  $\chi^2 = \chi^2_{min} + 1$

TABLE 7 Experimental values of the Two Photon Radiative Widths of the  $\eta$  and  $\eta'$ . The First Quoted Error is Statistical the Second Systematic.

$\Gamma_{\gamma\gamma}(\eta')$ (keV)	Experiment	Reference
5.4 $\pm 2.1$	$\Gamma(\eta'), BR(\eta' \rightarrow \gamma\gamma)$	[63]
5.8 $\pm 1.0 \pm 1.2$	MARK II	[64]
6.2 $\pm 1.1 \pm 0.8$	CELLO	[65]
5.0 $\pm 0.5 \pm 0.9$	JADE	[66]
3.8 $\pm 0.26 \pm 0.43$	PLUTO	[67]
5.0 $\pm 0.4 \pm 0.7$	TASSO	[68]
Average 4.5 $\pm 0.4$	all experiments	
$\Gamma_{\gamma\gamma}(\eta)$ (keV)	Experiment	Reference
1.0 $\pm 0.22$	Primakoff (DESY)	[69]
0.324 $\pm 0.046$	Primakoff (Cornell)	[70]
0.56 $\pm 0.12 \pm 0.09$	Crystal Ball	[1]
0.56 $\pm 0.05 \pm 0.08$	JADE	[1]
Average 0.56 $\pm 0.08$	Crystal Ball and JADE only	

61

TABLE 9 Predictions of Branching Ratios and  $\Gamma$  Radiative Widths for  $\psi(1450)$

Prediction	Experimental Value	Ref.
$BR(J/\psi \rightarrow \psi\gamma)$	$(8.6 \pm 2.0) \times 10^{-3}$	[61]
$BR(\psi \rightarrow K\bar{K}\pi)$ b)	$0.42 \pm 0.10$	$> (4.9 \pm 0.74) \times 10^{-3}$ a)
$BR(\psi \rightarrow \rho\gamma)$ c)	$(1.2 \pm 0.4) \times 10^{-2}$	-
$\Gamma_{\gamma\gamma}(\psi) BR(\psi \rightarrow K\bar{K}\pi)$	$4.3 \pm 1.6$ keV	$\leq 7$ keV 95 % CL [1]
$\Gamma_{\gamma\gamma}(\psi) BR(\psi \rightarrow \rho\gamma)$	$0.12 \pm 0.05$ keV	$\leq 8$ keV 95 % CL [1]
$BR(J/\psi \rightarrow \psi\gamma) BR(\psi \rightarrow \rho\gamma)$	$(1.0 \pm 0.4) \times 10^{-4}$	$\leq 1.5$ keV 95 % CL [68]
$BR(J/\psi \rightarrow \psi\gamma) BR(\psi \rightarrow \omega\gamma)$	$(1.1 \pm 0.3) \times 10^{-5}$	$(0.88 \pm 0.28 \pm 0.15) \times 10^{-4}$ d)
$BR(J/\psi \rightarrow \psi\gamma) BR(\psi \rightarrow \phi\gamma)$	$(1.2 \pm 0.4) \times 10^{-5}$	$(1.1 \pm 0.24 \pm 0.25) \times 10^{-4}$ e)
$\Gamma_{\rho\gamma}(\psi)$	1160 $\pm$ 350 keV	$2.1 \times 10^{-4}$ 90 % CL e)
$\Gamma_{\omega\gamma}(\psi)$	124 $\pm$ 38 keV	$2.3 \times 10^{-4}$ 90 % CL e)
$\Gamma_{\phi\gamma}(\psi)$	129 $\pm$ 39 keV	-

a) Lower limit given by assuming 100 % BR in  $K\bar{K}\pi$ .

b) Using the value  $(4.9 \pm 0.74) \times 10^{-3}$  for  $BR(\psi \rightarrow \rho\gamma) BR(\psi \rightarrow K\bar{K}\pi)$ . This is the weighted average of the MARK II, Crystal Ball and MARK III results presented in Ref. [61].

c) Using  $\Gamma_{\rho\gamma}(\psi)$  as given above and  $\Gamma(\psi) = 95 \pm 5$  MeV, corresponding to the weighted average of the values of the MARK III and DM2 Collaborations as quoted in Ref. [61].

d) Crystal Ball Collaboration.

e) MARK III Collaboration.

TABLE 10

$m_{\pi^+}$	$\nu$	Mass Scaling for $ \psi(0) ^2$
1330	0	$\mu^{3/2}$
1430	- 1/2	$\mu^2$
1520	-1	$\mu^3$

$\mu \equiv$  reduced mass

TABLE 12 Values of 'Effective' Flavour Amplitudes for Different Mixing Solutions

$x_{ef}$		$y_{ef}$		$z_{ef}$		Solution
$\eta$	$\eta'$	$\eta$	$\eta'$	$\eta$	$\eta'$	
0.67	0.50	-0.73	0.61	-0.14	-0.62	Ground states only with gluonium (Table 6)
0.75	0.43	-0.81	0.65	—	—	Ground states and first radial excitations without gluonium (Eqn (43))
0.78	0.44	-0.78	0.70	-0.09	-0.27	Ground states and first radial excitations with gluonium (Eqn (45))

TABLE 11 Flavour Mass Mixing Matrix in the Basis  $\psi_1^{ns}, \psi_2^{ns}, \psi_1^s, \psi_2^s, G$

$M_{1ns}^0 - 3 \Delta_1^{ns} + 2\alpha$	$(-3 \Delta_1^{ns} + 2\alpha)Y$	$\sqrt{2}\alpha Z_{11}$	$\sqrt{2}\alpha Z_{12}Y$	$\sqrt{2}B$
$(-3 \Delta_1^{ns} + 2\alpha)Y$	$M_{2ns}^0 - (3 \Delta_1^{ns} - 2\alpha)Y^2$	$\sqrt{2}\alpha Z_{12}Y$	$\sqrt{2}\alpha Z_{22}Y^2$	$\sqrt{2}BY$
$\sqrt{2}\alpha Z_{11}$	$\sqrt{2}\alpha Z_{12}Y$	$M_{1s}^0 - 3 \Delta_1^s + \alpha Z_{11}^2$	$(-3 \Delta_1^s + \alpha Z_{12}^2)Y$	$Z_{12}B$
$\sqrt{2}\alpha Z_{12}Y$	$\sqrt{2}\alpha Z_{22}Y^2$	$(-3 \Delta_1^s + \alpha Z_{12}^2)Y$	$M_{2s}^0 - (3 \Delta_1^s - \alpha Z_{22}^2)Y^2$	$Z_{22}BY$
$\sqrt{2}B$	$\sqrt{2}BY$	$Z_{12}BY$	$Z_{22}BY$	$M_G$

TABLE 13 Values of  $\Gamma_{\gamma\gamma}(n')$  (keV) for Different Mixing Solutions

FC	IC	Solution
5.5	17.6	Ground states only with gluonium (Table 6)
5.3	17.9	Ground states and first radial excitations without gluonium (Eqns (43))
5.9	20.3	Ground states and first radial excitations with gluonium (Eqns (45))

Experiment:  $4.5 \pm 0.4$  keV

TABLE 14

Experimental Values of the Two Photon Radiative Widths of the Tensor Mesons  $f$ ,  $f'$ ,  $A_2$ .  
The First Quoted Error is Statistical the Second Systematic.

$\Gamma_{\gamma\gamma}(f)$ (keV)	Experiment	Ref.
$2.3 \pm 0.5 \pm 0.35$	PLUTO	[77]
$3.6 \pm 0.3 \pm 0.5$	MARK II	[78]
$3.2 \pm 0.2 \pm 0.6$	TASSO	[79]
$2.7 \pm 0.2 \pm 0.6$	Crystal Ball	[80]
$2.5 \pm 0.1 \pm 0.5$	CELLO	[81]
$2.3 \pm 0.2 \pm 0.5$	JADE	[1]
<u>Average</u>		<u><math>2.85 \pm 0.26</math></u>
$\Gamma_{\gamma\gamma}(f')$ (keV)		
<u><math>0.11 \pm 0.02 \pm 0.04</math></u>	TASSO	[14]
$\Gamma_{\gamma\gamma}(A_2)$ (keV)		
$0.77 \pm 0.18 \pm 0.27$	Crystal Ball	[80]
$0.81 \pm 0.19 \pm 0.27$	CELLO	[65]
$0.84 \pm 0.07 \pm 0.15$	JADE	[1]
<u>Average</u>		<u><math>0.82 \pm 0.13</math></u>

TABLE 15 Flavour Mixing Amplitudes for  $f, f', \theta$ .  
FC Quark Model

State	x	y	z	Solution
f	0.998	0.068	-0.016	non rel.
f'	0.065	-0.998	0.01	(Eqn (16))
$\theta$	0.016	0.011	0.9998	
f	0.987	0.061	-0.147	non rel.
f'	0.071	-0.994	0.081	with SU(2) breaking [82]
$\theta$	0.141	0.088	0.986	
f	0.986	0.067	-0.155	with relativistic corrections [7]
f'	0.079	-0.993	0.094	
$\theta$	0.148	0.1011	0.984	

TABLE 16 Experimental, Fitted and Predicted Widths for the  
Strong Decays  $T \rightarrow PP, T \rightarrow VP$

Process	Experimental Width (MeV) a)	Theoretical Width (MeV)
$f \rightarrow \pi\pi$	$149 \pm 17$	145 (fit)
$f \rightarrow K\bar{K}$	$5.2 \pm 0.7$	5.1 (fit)
$f' \rightarrow \pi\pi$	$0.8 \pm 0.3$	1.3 (fit)
$f' \rightarrow K\bar{K}$	$59 \pm 10$ b)	50 (fit)
$f' \rightarrow \eta\eta$	-	7 (pred.)
$A_2 \rightarrow K\bar{K}$	$5.3 \pm 0.6$	6.4 (pred.)
$A_2 \rightarrow \eta\pi$	$16.0 \pm 1.5$	20 (pred.)
$K^{**} \rightarrow K\pi$	$45 \pm 5$	73 (pred.)
$K^{**} \rightarrow K\eta$	$2.9 \pm 1.7$ [83]	0.6 (pred.)
$A_2 \rightarrow \rho\pi$	$77 \pm 4$	77 Input
$K^{**} \rightarrow K\rho$	$8.8 \pm 1.0$	5.6 (pred.)
$K^{**} \rightarrow K\omega$	$4.2 \pm 1.6$ [83]	1.5 (pred.)
$K^{**} \rightarrow K^*\pi$	$25 \pm 3$	19 (pred.)

a) Unless otherwise indicated all experimental values are taken from Ref. [31].

b) Total width corrected by subtracting  $\Gamma_{\pi\pi}(f')$ ,  $\Gamma_{\eta\eta}(f')$  as described in the text.

## Figure Captions

Fig. 1 Coupling constant definitions in the Ge11-Mann Sharp Wagner model.  
 a)  $V \rightarrow e^+e^-$ , b)  $\omega \rightarrow \pi^0\gamma$ , c)  $\pi^0 \rightarrow \gamma\gamma$

Fig. 2 Diagrams contributing to radiative decay processes in the Van Royen Weisskopf model.

a)  $V \rightarrow e^+e^-$ , b)  $V(P) \rightarrow P(V)\gamma$ , c)  $P \rightarrow \gamma\gamma$

Fig. 3 Quark annihilation diagrams contributing to  $\Gamma_{\gamma\gamma}(P)$  in different models.

a) Triangle graph giving the axial anomaly in the current algebra calculation.  
 b) Quarkonium annihilation diagram.

Fig. 4 a) Flavour mixing amplitude via two gluon exchange in QCD.  
 b) Flavour mixing amplitude via two W exchange in the weak interaction.

Fig. 5 Lowest order QCD diagrams contributing to the elements of the mass mixing matrix  $\hat{M}(22)$ .

Fig. 6 Lowest order QCD diagrams illustrating the factorisation between amplitudes contributing to  $J/\psi$  radiative decays and the corresponding elements of the mass mixing matrix.

Fig. 7 Duality diagrams used to estimate strong decay amplitudes.

a)  $M \rightarrow M_1 \bar{M}_1$  b)  $\pi^+ p \rightarrow \eta(n^+)n$

Fig. 8 The ratio of the experimental to predicted values of  $\Gamma_{\gamma\gamma}(n^+)$  in gauge integer charge quark models as a function of the effective gluon mass  $m_g$ .

A.  $p_T^{n^+} \leq 0.1$  GeV

B.  $p_T^{n^+} \leq 0.2$  GeV

C. No  $p_T^{n^+}$  cut

TABLE 17

System	$\Delta / \bar{\Gamma}$
$1S_0$ positronium	$2.6 \times 10^{-3}$
$\eta_b$	0.17
$\eta_c$	0.23
$\eta'$	0.52
$\eta$	0.38
$\pi^0$	0.49

Fig. 9 Amplitude of  $|G\rangle$  in the  $f, f', \theta$  as a function of the parameter  $\gamma$ .  
(See (46)).

Fig. 10 The two photon radiative width of the  $\theta$  as a function of  $\gamma$ .  
(See (46)).

Fig. 11  $\Gamma_{\gamma\gamma}(\theta) BR(\theta \rightarrow K\bar{K})$  as a function of  $\gamma$  (see (46)).

Fig. 12 The IC model predictions as a function of  $\gamma$  (see (46)) compared  
with the experimental values for:  
a)  $\Gamma_{K\bar{K}}(f)$ , b)  $\Gamma_{K\bar{K}}(f')$ .

### References

1. J.E. Olsson in Proceedings of the Fifth International Workshop on Photon Photon Collisions, Aachen 1983, Ed. Ch. Berger, Lecture Notes in Physics 191, Springer Verlag Heidelberg, 45-73
- A. Cordier in Proceedings of the Sixth International Workshop on Photon Photon Collisions, Lake Tahoe, Calif., September 1984, Ed. R.L. Lahder, World Scientific Singapore 1985
2. H. Suura, T.F. Walsh and B.L. Young, Lett. Nuovo Cimento 4, 505 (1972)
3. M.S. Chanowitz, Phys. Rev. Lett. 35, 977 (1975)
4. M.S. Chanowitz, Phys. Rev. Lett. 44, 59 (1980)
5. L. Bergström, H. Snellman and G. Tengstrand, Phys. Lett. 80B, 242 (1979)  
L. Bergström, H. Snellman and G. Tengstrand, Phys. Lett. 82B, 419 (1979)
6. R. McClary and N. Byers, Phys. Rev. D28, 1692 (1983)  
P. Falkensteiner, H. Grosse and F. Schöberl, Phys. Lett. 148B, 194 (1984)
7. L. Bergström, G. Huith and H. Snellman,  
Z. Phys. C Particles and Fields 16, 263 (1983)
8. H.J. Schnitzer, Nucl. Phys. B207, 131 (1982)
9. J.L. Rosner, Phys. Rev. D27, 1101 (1983)
10. J.L. Rosner and S.F. Tuan, Phys. Rev. D27, 1544 (1983)
11. H. Fritzsche and J.D. Jackson, Phys. Lett. 66B, 365 (1977)
12. D.P. Stanley and D. Robson, Phys. Rev. D21, 3180 (1980)
13. J.L. Rosner, Phys. Rev. D24, 1347 (1981)
14. TASSO Coll., M. Althoff et al., Phys. Lett. 121B, 216 (1983)
15. M. Han and Y. Nambu, Phys. Rev. 139, 1006 (1965)
16. JADE Coll., W. Bartel et al., Phys. Lett. 107B, 163 (1981)
17. TASSO Coll., R. Brandelik et al., Phys. Lett. 107B, 290 (1981)
18. MAC Coll., E. Fernandez et al., Phys. Rev. Lett. 54, 95 (1985)
19. J.C. Pati and A. Salam, Phys. Rev. D8, 1240 (1973)
20. J.C. Pati and A. Salam, Phys. Rev. D10, 275 (1974)

46. J.J. Sakurai, Phys. Rev. 132, 434 (1963)
47. Ya. B. Zel'dovich and A.D. Sakharov, J. Nucl. Phys. (USSR) 4, 395 (1966), Sov. J. Nucl. Phys. 4, 283 (1967)
48. H.F. Jones and M.D. Scadron, Nucl. Phys. B155, 409 (1979)
49. H. Suura and M. Kuroda, Prog. Theor. Phys. 54, 1513 (1975)
50. D. Hitlin in Proceedings of the 1983 International Symposium on Lepton and Photon Interactions at High Energies, Cornell University
51. S. Okubo and K. Jagannathan, Phys. Rev. D15, 177 (1977)
52. S. Okubo, Phys. Lett 5, 165 (1963)
53. G. Zweig, CERN pre-print 1964 (unpublished)
54. J. Iizuka, Prog. Theor. Phys. Suppl. 37-38, 21 (1966)
55. W.D. Apel et al., Phys. Lett. 83B, 131 (1979)
56. K. Ishikawa, A. Sato, G. Schierholz and M. Teper, Contributed Paper C-270, 1983, International Symposium on Lepton and Photon Interactions at High Energies, Cornell University
57. M. Chanowitz and S. Sharpe, Nucl. Phys. B222, 211 (1983)
58. J.M. Cornwall and A. Soni, Phys. Lett. 120B, 431 (1983)
59. I. Cohen, N. Isgur and H.J. Lipkin, Phys. Rev. Lett. 48, 1074 (1982)
60. H. Fritzsche and P. Minkowski, Nuovo Cimento 30A, 393 (1975)
61. N. Isgur, Phys. Rev. D13, 122 (1976)
62. A.L. Spadafora, University of Illinois at Urbana, Champaign pre-print UI-HEPG-84-3
63. J. Perrier. Invited talk presented at the International Conference "Physics in Collision", Santa Cruz, California, August 1984; SLAC-PUB-3436, September 1984
64. J.D. Jackson, Proceedings of the Summer Institute on Particle Physics, SLAC 1976, LBL-5500, 1976
65. D. Binnie et al., Phys. Lett. 83B, 141 (1979)
66. MARK II Coll., G. Abrams et al., Phys. Rev. Lett. 43, 477 (1979)
67. CELLO Coll., H.-J. Behrend et al., Phys. Lett 114B, 378 (1982), E 125B, 518 (1983)

21. R.N. Mohapatra, J.C. Pati and A. Salam, Phys. Rev. D13, 1733 (1976)
22. G. Rajasekaran and S.D. Rindani, Prog. Theor. Phys. 67, 1505 (1982)
23. A. Yu. Ignat'ev et al., Theor. Math. Phys. (USSR) 47, 373 (1981)
24. T. Jayaraman, G. Rajasekaran and S.D. Rindani, Phys. Lett. 119B, 215 (1982)
25. A. Janah and M. Üzer, Univ. of Maryland, pre-print, 81-221 (1981)
26. R.M. Godbole et al., Phys. Lett. 142B, 91 (1984)
27. H.J. Lipkin, Nucl. Phys. B155, 104 (1979)
28. J.S. Bell and R. Jackiw, Nuovo Cimento LXA, 47 (1969)
29. S.L. Adler, Phys. Rev. 177, 2426 (1969)
30. M. Gell-Mann, D. Sharp and M.G. Wagner, Phys. Rev. Lett 8, 261 (1962)
31. Review of Particle Properties, Phys. Lett. 111B (1982)
32. R.H. Dalitz and D.G. Sutherland, Nuovo Cimento XXXVIII, 1777 (1965)
33. R. Van Royen and V.F. Weisskopf, Nuovo Cimento LA, 617 (1967)
34. J.H. Field in Proceedings of the International Europhysics Conference on High Energy Physics, Brighton 1983, page 168
35. R.K. Bhaduri, L.E. Cohler and Y. Nogami, Nuovo Cimento 65A, 376 (1981)
36. S. Godfrey and N. Isgur, Phys. Rev. D32, 189 (1985)
37. N. Isgur, Phys. Rev. D13, 129 (1976), D23, 817 (E)
38. V.M. Budnev and A.E. Kaloshin, Phys. Lett. 86B, 351 (1979)
39. J.E. Paschalis and G.J. Gounaris, Nucl. Phys. B222, 473 (1983)
40. A. de Rújula, H. Georgi and S.L. Glashow, Phys. Rev. 120, 147 (1975)
41. R. Barbieri, R. Gatto and E. Remiddi, Phys. Lett. 106B, 497 (1981)
42. G.P. Lepage in Proceedings of the 1983 International Symposium on Lepton and Photon Interactions at High Energies, Cornell University, page 565
43. J.M. Jauch and F. Röhrlich. The Theory of Photons and Electrons, Addison-Wesley Publishing Co. Inc., Cambridge, Mass., (1955)
44. C. Quigg and J.L. Rosner, Phys. Rep. 56C, 167 (1979)
45. S. Samuel and K.J.M. Moriarty 'On the Constituent Masses of Quarks', City College of New York Preprint, March 1985



66. JADE Coll., W. Bartel et al., Phys. Lett. 113B, 190 (1982)
67. PLUTO Coll., Ch. Berger et al., Phys. Lett. 142B, 455 (1984)
68. TASSO Coll., M. Althoff et al., Phys. Lett. 147B, 487 (1984)
69. C. Bemporad et al., Phys. Lett. 25B, 380 (1967)
70. A. Browman et al., Phys. Rev. Lett. 32, 1067 (1974)
71. J.H. Field, Nucl. Phys. B168, 477 (1980), E B176, 545 (1980)
72. M. Frank and P.J. O'Donnell, Phys. Lett. 133B, 253 (1983)
73. M. Frank and P.J. O'Donnell, Phys. Rev. D29, 921 (1984)
74. M. Frank and P.J. O'Donnell, Phys. Lett. 144B, 451 (1984)
75. A. Martin, pre-print CERN TH-3763 (November 1983)
76. N. Wermes, pre-print SLAC-PUB-3312, Proceedings of the 19th Rencontre de Moriond, Vol. 2 'New Particle Production', page 663. Editions Frontières 1984, Ed. J. Tran Thanh Van
77. PLUTO Coll., Ch. Berger et al., Phys. Lett. 94B, 254 (1980)
78. MARK II Coll., A. Roussarie et al., Phys. Lett. 105B, 304 (1981)
79. TASSO Coll., R. Brandelik et al., Z. Phys. C Particles and Fields 10, 117 (1981)
80. Crystal Ball Coll., C. Edwards et al., Phys. Lett. 105B, 304 (1981)
81. CELLO Coll., H.-J. Behrend et al., Z. Phys. C Particles and Fields 23, 223 (1984)
82. N. Isgur, H.R. Rubinstein, A. Schwimer and H.J. Lipkin, Phys. Lett. 89B, 79 (1979)
83. J.H. Field, T. Hendricks, O. Piccioni and P. Yager, Phys. Lett. 24B, 638 (1967)
84. R.L. Jaffe, Phys. Rev. D15, 281 (1977)
85. B.A. Li and Q.X. Shen, Phys. Lett. 126B, 125 (1982)
86. F.E. Close, Phys. Rev. D27, 311 (1983)
87. E.B. Daily et al., Phys. Rev. Lett. 48, 375 (1982)
88. B. Durand and L. Durand, Phys. Rev. D30, 1904 (1984)
89. R.P. Worden, Phys. Lett. 52B, 87 (1974)
90. K.H. Chan, S.K. Han and J.K. Kim, Phys. Rev. D27, 684 (1983)
91. S.J. Brodsky et al., Phys. Rev. D19, 1418 (1979)  
K. Kajantie and R. Raitio, Phys. Lett. 87B, 133 (1979)
92. J.A. Bagger and J.F. Gunion, Phys. Rev. D29, 40 (1984)
93. P. Astbury et al., Phys. Lett. 152B, 419 (1985)
94. T. Jayaraman and S.D. Rindani, University of Madras, pre-print 1984  
T. Jayaraman, Ph. D. Thesis University of Madras 1983
95. C. Kourkouvelis et al., Z. Phys. C Particles and Fields C16, 101 (1982)

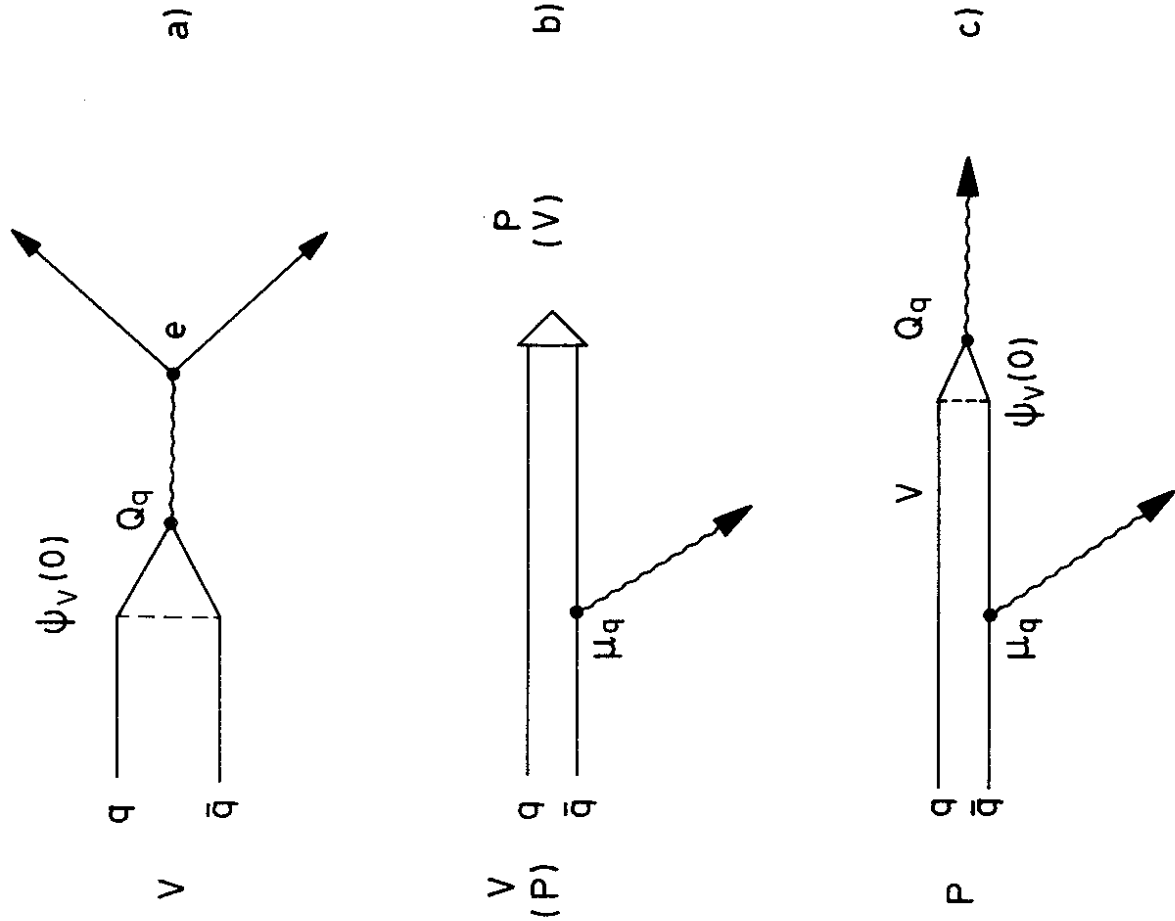


Fig. 2

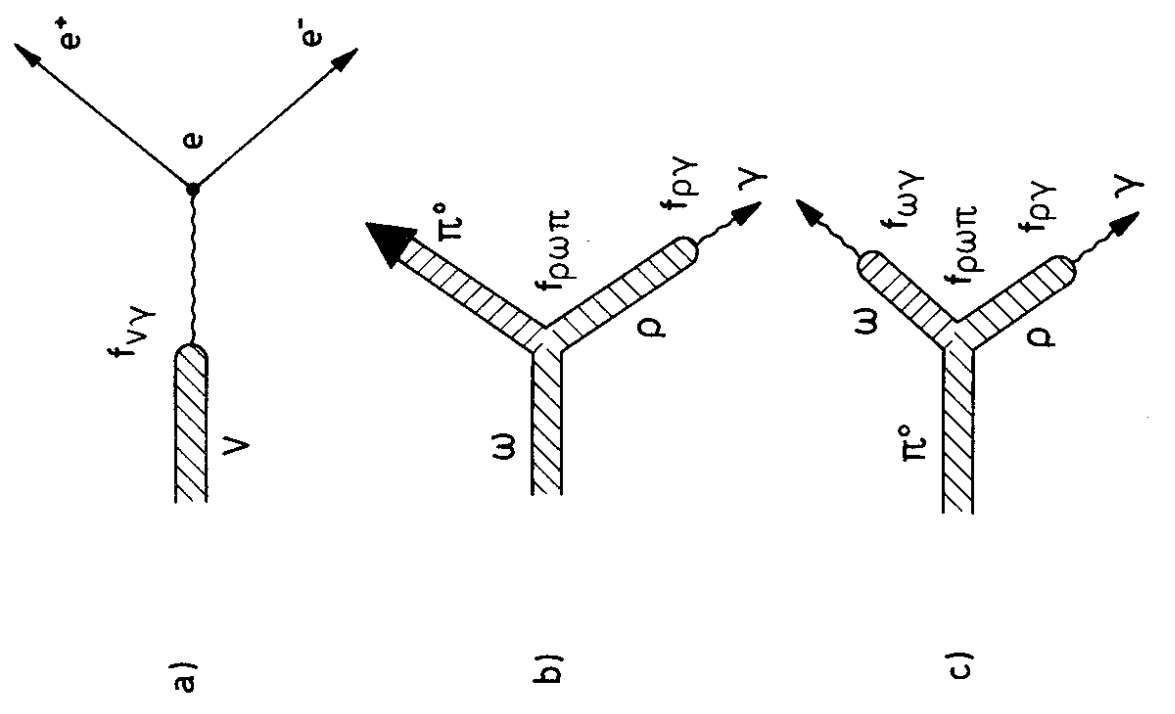


Fig. 1

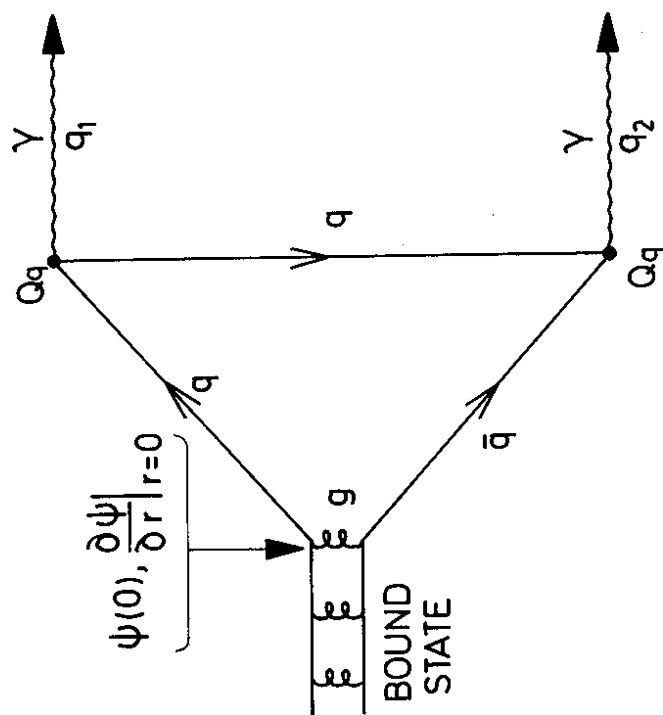
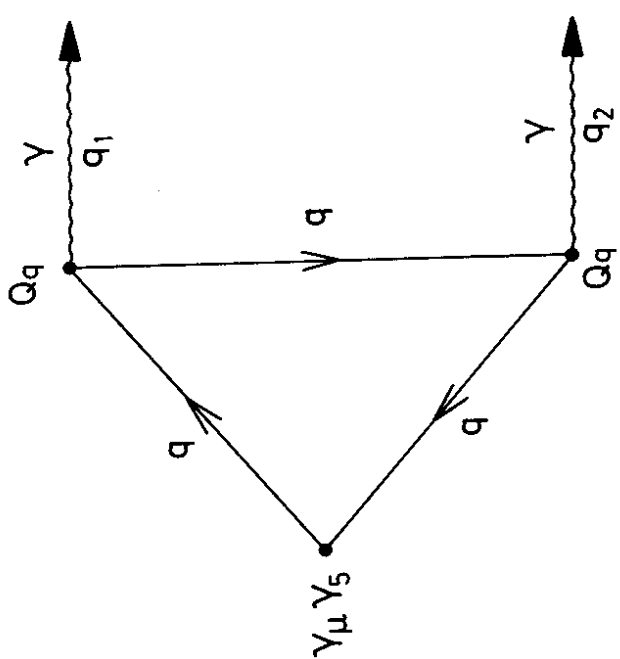


Fig. 3

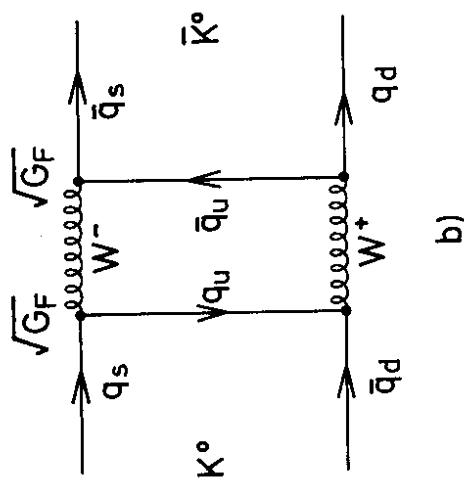
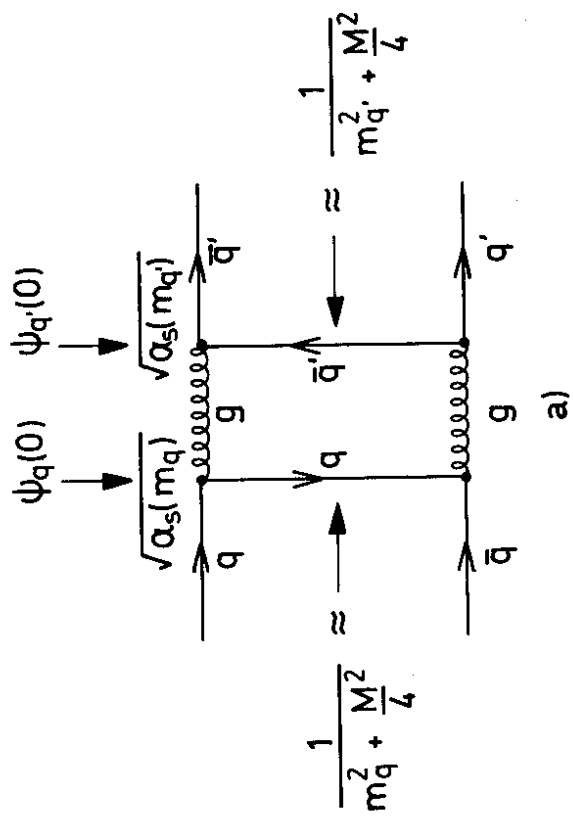
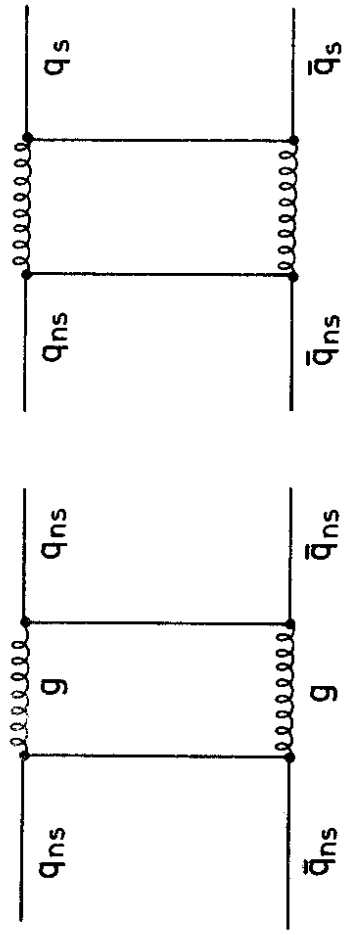
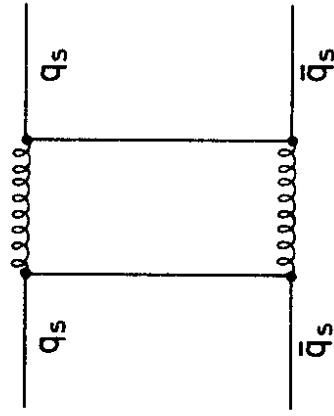


Fig. 4



$\alpha$

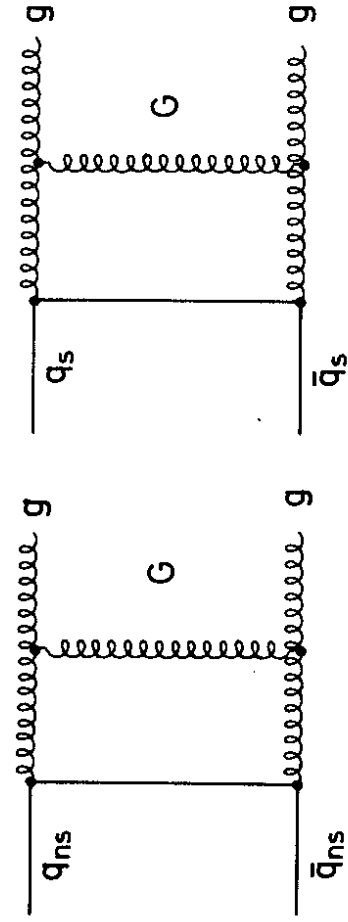
$Z\alpha$



$\alpha$

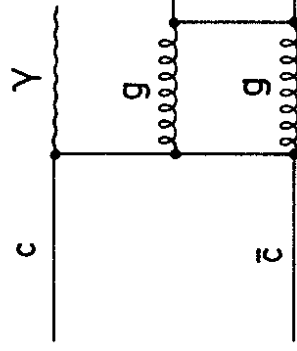
$Z\alpha$

$Z^2\alpha$



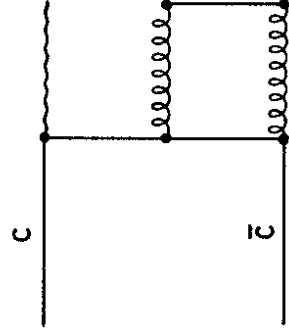
$\beta$

$Z\beta$



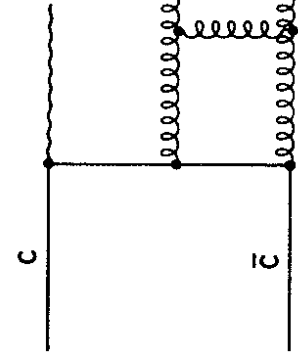
$\approx$

$= \alpha$



$\approx$

$= Z\alpha$



$\approx$

$= \beta$

$\beta$

$Z\beta$

Fig. 6

Fig. 5

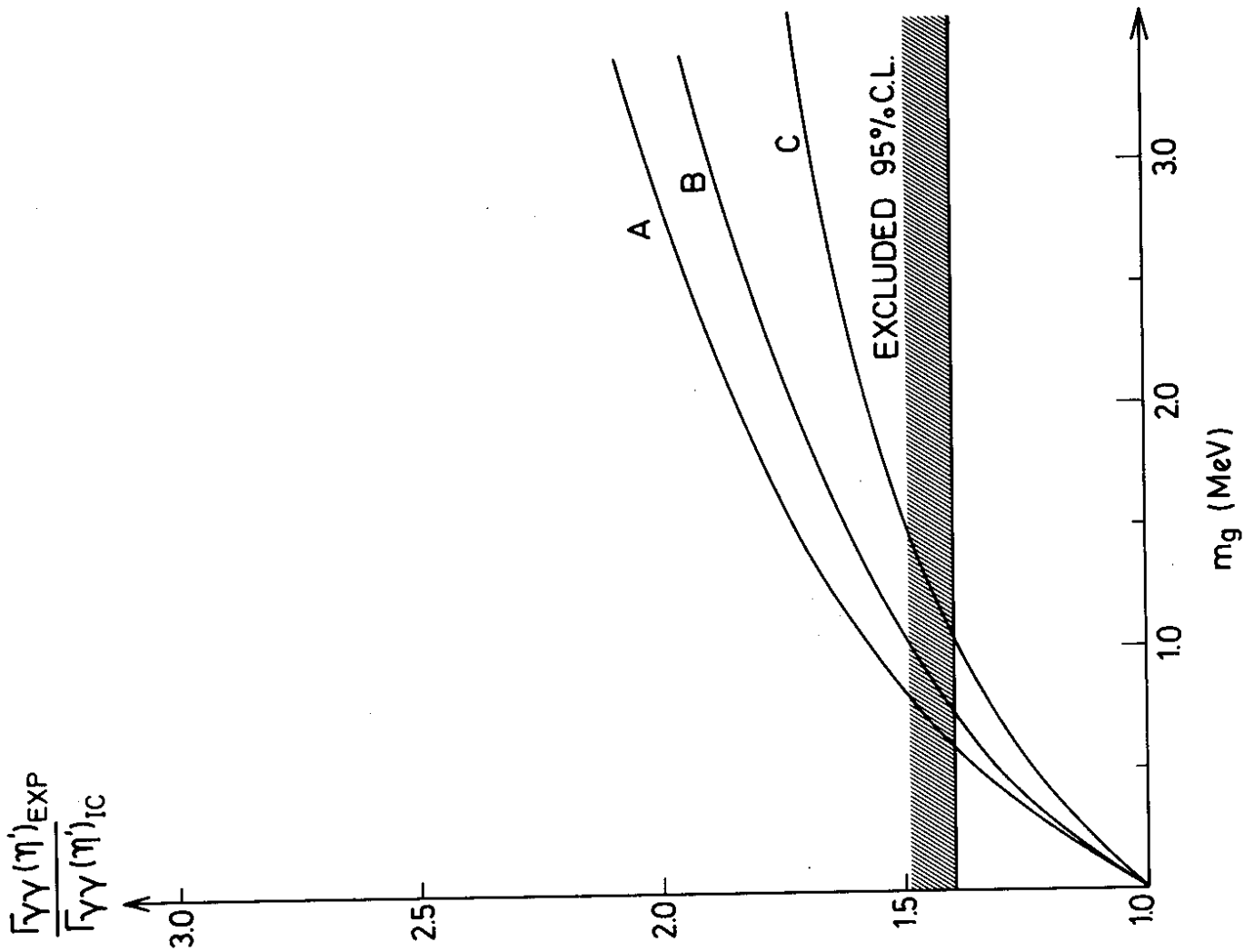
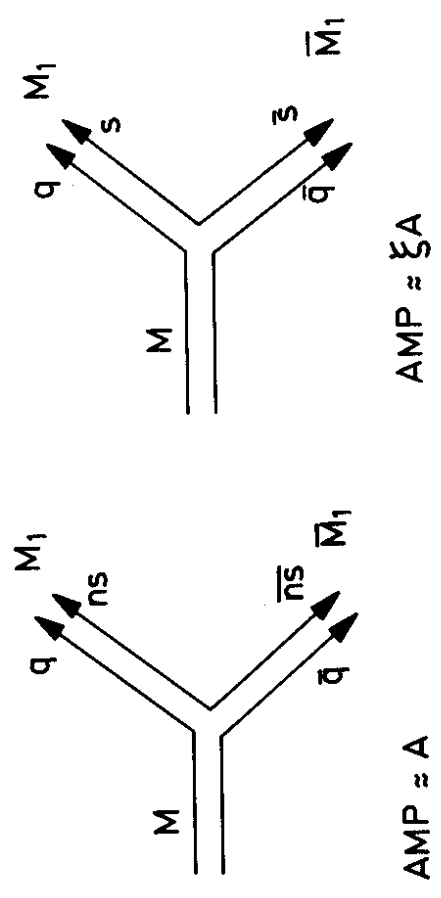


Fig. 8



a)

b)

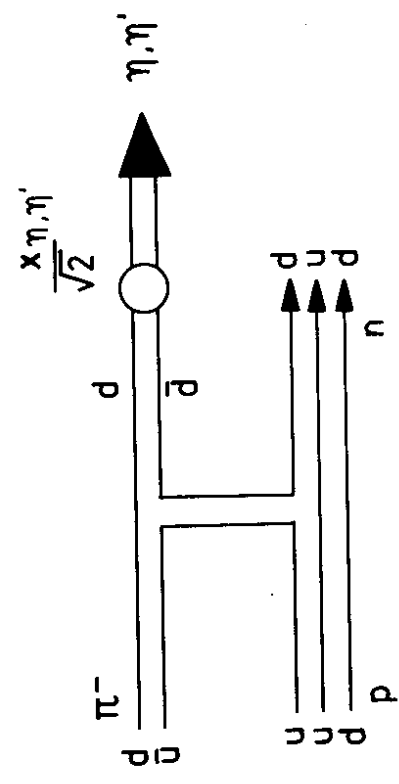


Fig. 7

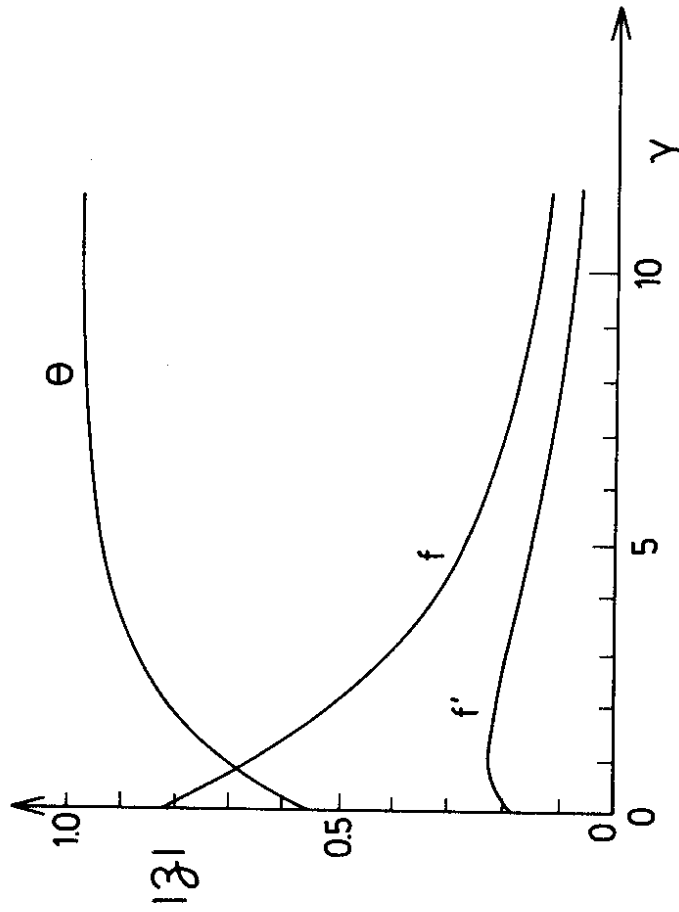


Fig. 9

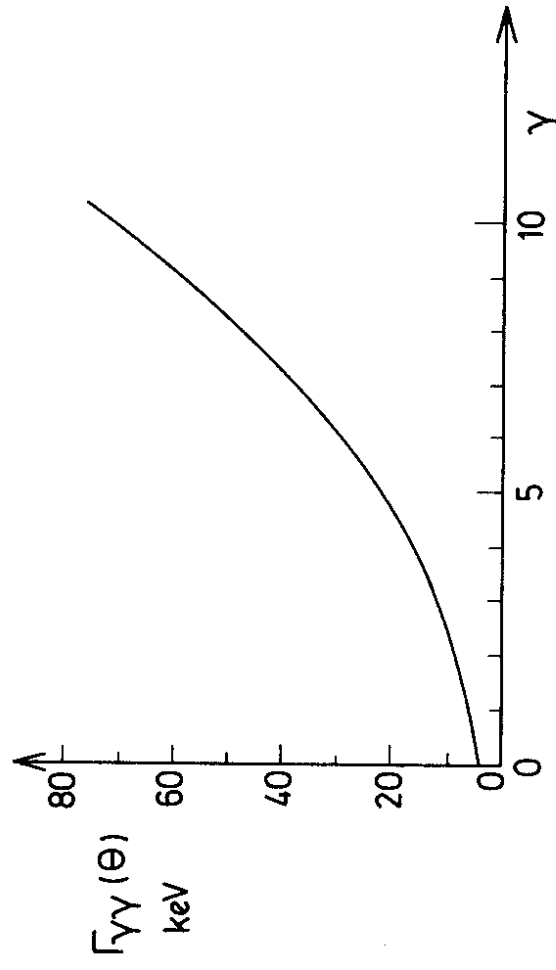


Fig. 10

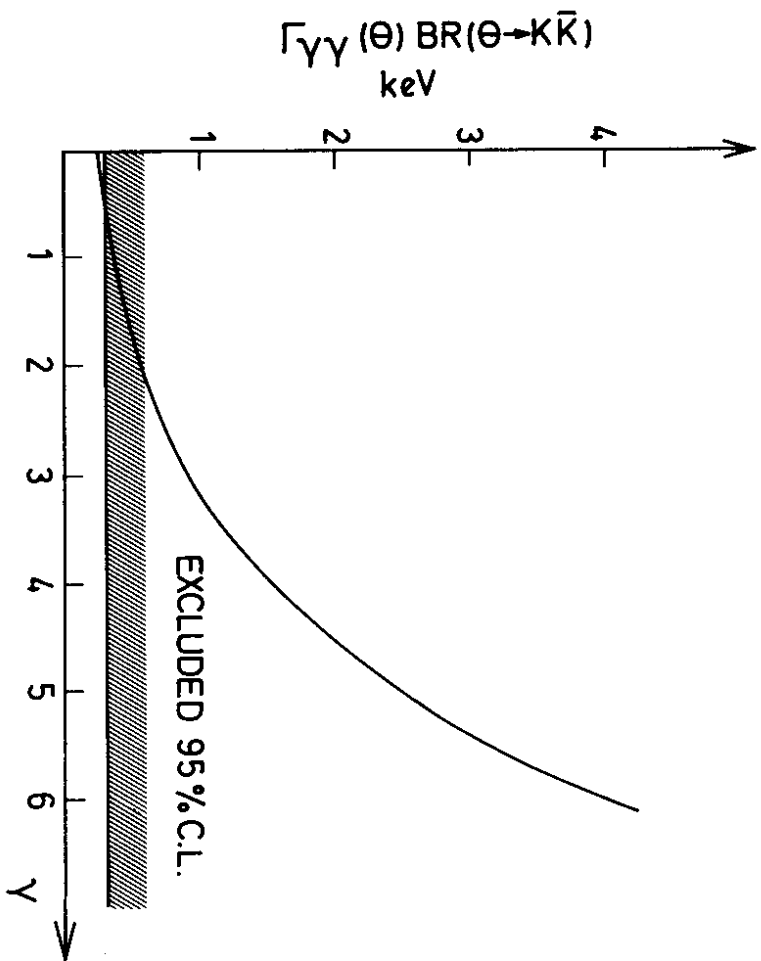


Fig. 11

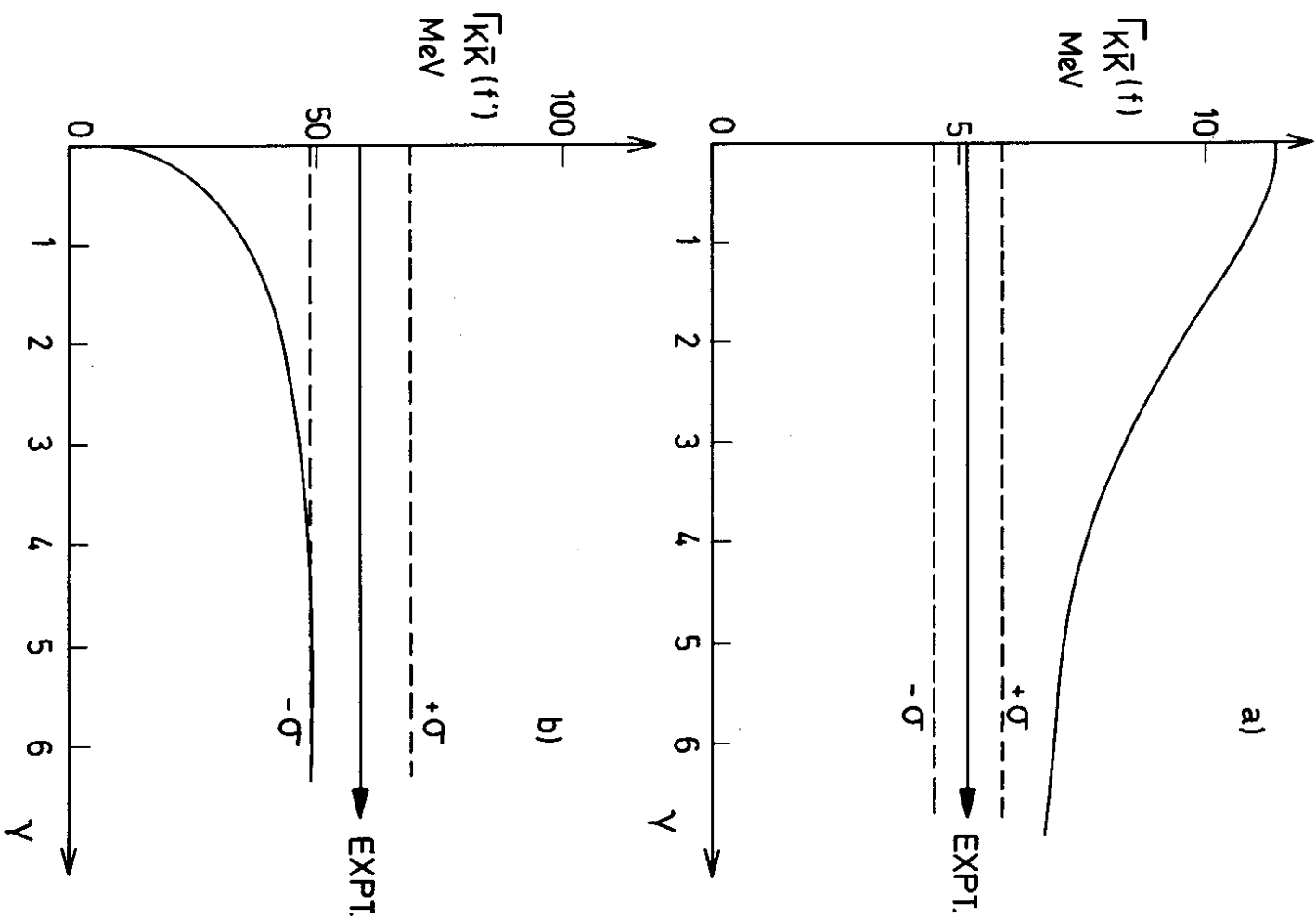


Fig. 12